JACS
JOURNAL OF THE AMERICAN CHEMICAL SOCIETY

Article

pubs.acs.org/JACS

Controlling the Architecture, Coordination, and Reactivity of Nanoparticle Coating Utilizing an Amino Acid Central Scaffold

Naiqian Zhan,[†] Goutam Palui,[†] Anshika Kapur,[†] Valle Palomo,[‡] Philip E. Dawson,[‡] and Hedi Mattoussi*[,†]

[†]Department of Chemistry and Biochemistry, Florida State University, Tallahassee, Florida 32306, United States

[‡]Department of Chemistry, The Scripps Research Institute, La Jolla, California 92037, United States

Supporting Information

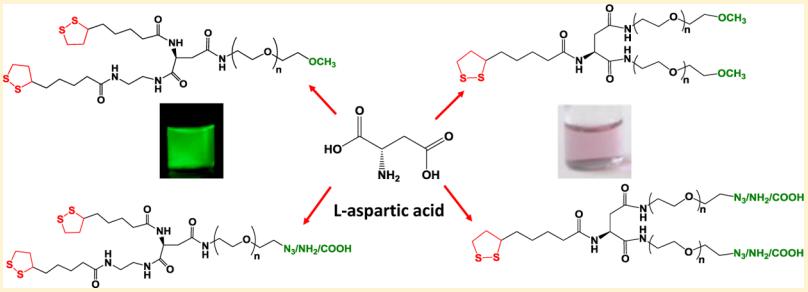

ABSTRACT: We have developed a versatile strategy to prepare a series of multicoordinating and multifunctional ligands optimized for the surface-functionalization of luminescent quantum dots (QDs) and gold nanoparticles (AuNPs) alike. Our chemical design relies on the modification of L-aspartic acid precursor to controllably combine, through simple peptide coupling chemistry, one or two lipoic acid (LA) groups and poly(ethylene glycol) (PEG) moieties in the same ligand. This route has provided two sets of modular ligands: (i) bis(LA)-PEG, which presents two lipoic acids (higher coordination) appended onto a single end-functionalized PEG, and (ii) LA-$(PEG)_2$ made of two PEG moieties (higher branching, with various end reactive groups) appended onto a single lipoic acid. These ligands are combined with a new photoligation strategy to yield hydrophilic and reactive QDs that are colloidally stable over a broad range of conditions, including storage at nanomolar concentration and under ambient conditions. AuNPs capped with these ligands exhibit excellent stability in various biological conditions and improved resistance against NaCN digestion. This route also provides compact nanocrystals with tunable surface reactivity. As such, we have covalently coupled QDs capped with bis(LA)-PEG-COOH to transferrin to facilitate intracellular uptake. We have also characterized and quantified the coupling of dye-labeled peptides to QD surfaces using fluorescence resonance energy transfer interactions in QD−peptide−dye assemblies.

INTRODUCTION

In the past decade, inorganic nanocrystals, specifically gold nanoparticles (AuNPs) and semiconductor quantum dots (QDs), have generated great interest for applications in several areas of biology and medicine.[1−18] This stems from their unique sets of physical and chemical properties that exhibit size-, shape-, and composition-dependence. For example, metallic AuNPs show size- and shape-dependent surface plasmon resonance (SPR) absorption ranging from the visible to the near-infrared (NIR).[19−24] Similarly, some of the properties of semiconductor QDs including broad excitation, narrow and tunable emission across the visible and near-IR spectrum, high two-photon action cross-section, and superior photochemical stability account for their widespread applications as biological tagging and sensing agents.[3,7,25−29] However, typical synthesis of high-quality QDs (via "hot injection" routes) with narrow size distribution and control over size and core crystallinity provides nanocrystals that are capped with hydrophobic organic ligands.[30−36] These materials are exclusively soluble in hydrophobic solvents (such as toluene or hexane); this limits one's ability to integrate them with biomolecules, or introduce them into live cells. Therefore, an additional surface-modification with tailor-made ligands is required to render the nanocrystals stable in buffer media and biocompatible.[14,37−39]

Several strategies including silica coating, encapsulation, and ligand exchange have been reported for preparing biocompatible QDs.[40−53] Among those routes, ligand exchange that relies on the substitution of the native surface cap with hydrophilic coordinating ligands offers a few key advantages. This strategy is easy to implement and provides compact nanocrystals in aqueous media. It also permits easy introduction of specific reactive functionalities on the nanocrystal surfaces, for further modification with target biomolecules.[41,45,46,49,54−57] Several modular ligands bearing thiol, amine, pyridine, and imidazole as anchoring groups have been recently documented in the literature.[58−61] Among these, multidentate thiolated ligands, such as derivatives of dihydrolipoic acid (DHLA), provide enhanced colloidal stability to QDs (e.g., CdSe−ZnS) in

Received: October 3, 2015
Published: November 30, 2015

DOI: 10.1021/jacs.5b10359
J. Am. Chem. Soc. 2015, 137, 16084−16097

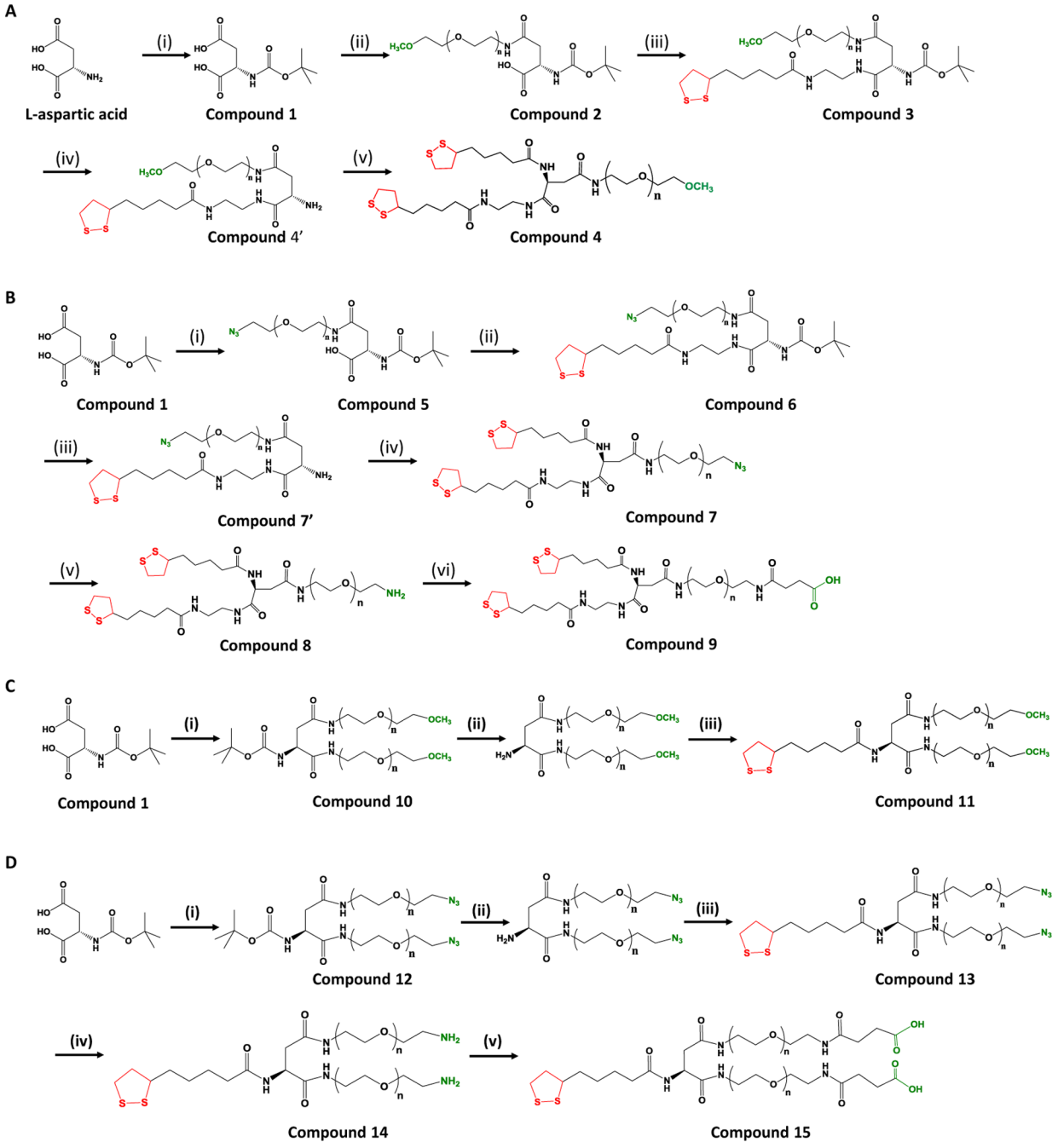

Figure 1. Schematic representation of the chemical structures and synthetic steps used to prepare the various ligands including: (A) bis(LA)PEG-OCH_3, (i) Boc_2O (di-*tert*-butyl dicarbonate); (ii) NH_2-PEG-OCH_3, DCC (*N*,*N*′-dicyclohexylcarbodiimide); (iii) LA-ethylenediamine, DCC, HOBt·H_2O (hydroxybenzotriazole monohydrate); (iv) 4 M HCl in dioxane; (v) LA (lipoic acid), DCC, DMAP (4-dimethylaminopyridine); only one isomer in step (ii) is shown (as a representative compound). (B) bis(LA)-PEG-N_3/NH_2/COOH, (i) NH_2-PEG-N_3, DCC; (ii) LA-ethylenediamine, DCC, HOBt·H_2O; (iii) 4 M HCl in dioxane; (iv) LA (lipoic acid), DCC, DMAP; (v) PPh_3 (triphenylphosphine), H_2O; (vi) succinic anhydride, Et_3N. (C) LA-$(PEG\text{-}OCH_3)_2$, (i) NH_2-PEG-OCH_3, DCC, HOBt·H_2O; (ii) 4 M HCl in dioxane; (iii) LA (lipoic acid), DCC, HOBt·H_2O. (D) LA-$(PEG\text{-}N_3/NH_2/COOH)_2$, (i) NH_2-PEG-N_3, DCC, HOBt·H_2O; (ii) 4 M HCl in dioxane; (iii) LA (lipoic acid), DCC, HOBt·H_2O; (iv) PPh_3, H_2O; (v) succinic anhydride, Et_3N.

aqueous media as compared to those presenting monodentate coordinating groups, due to the strong affinity of thiol to the zinc-rich QD surface and higher coordination of dithiol groups. Over the past decade, a variety of DHLA-based ligands have been synthesized and tested, confirming the benefits of cooperative coordination onto the ZnS-overcoated QDs.[46,50,51,60,62−65] The enhanced binding affinity of multi-thiol-appended ligands to AuNPs and AuNRs has also been reported.[66−68] To further exploit these effects, several groups have explored the possibility of using polymeric ligands instead, even though these can increase the hydrodynamic size of nanoparticles in buffer media.[41,46,48,55,61] One of the challenges in designing the ligands (either polymeric or molecular scale) is the versatility and scalability of the synthetic scheme. Specifically, factors that need to be taken into consideration

DOI: 10.1021/jacs.5b10359
J. Am. Chem. Soc. 2015, 137, 16084−16097

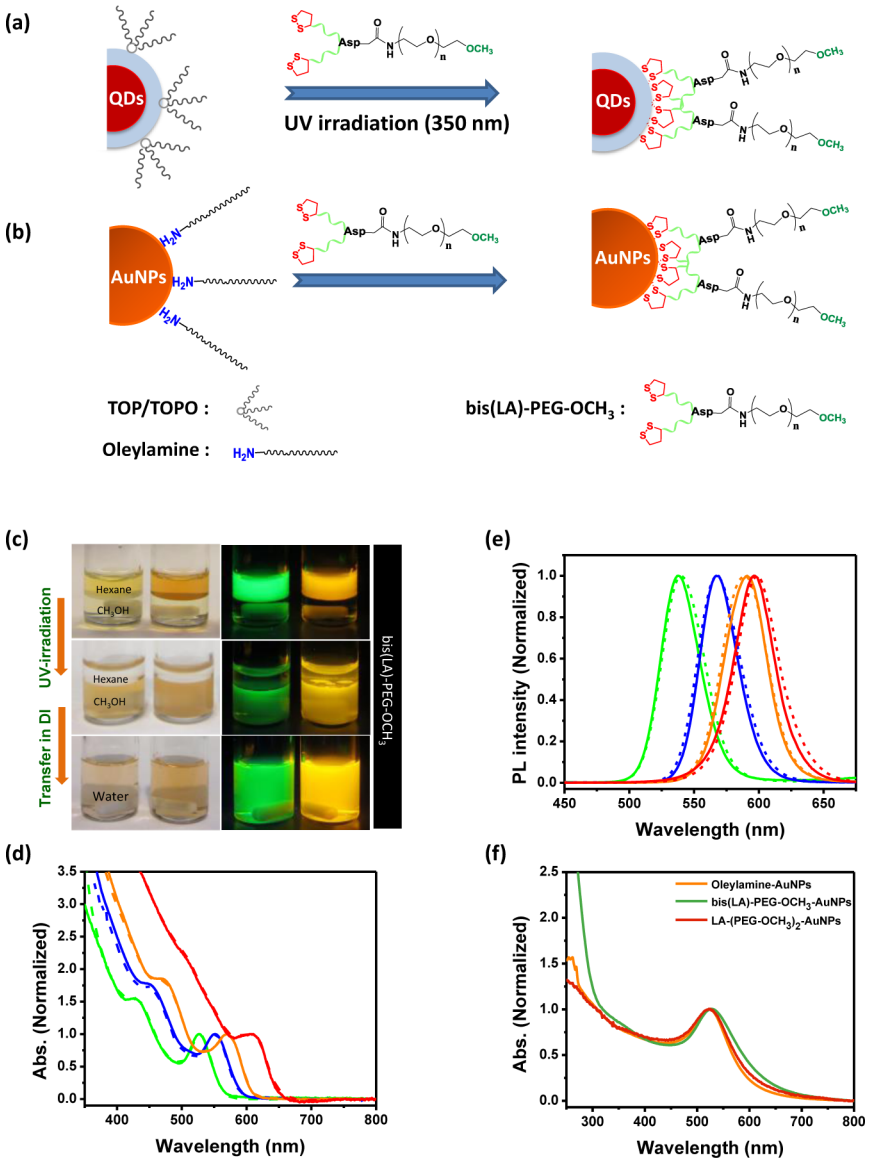

Figure 2. Schematic representation of the ligand exchange of hydrophobic (a) TOP/TOPO-QDs (via UV irradiation) and (b) oleylamine-AuNPs (without UV irradiation) with bis(LA)-PEG-OCH_3 ligand. (c) White light and fluorescence images of two different size QDs, showing nanocrystals in hexane (before irradiation, top images) and in methanol (after irradiation, middle images). The bottom images show QDs dispersed in DI water. (d) UV−vis and (e) PL spectra of the various sets of QDs (λ_{em} = 540, 567, 590, 598 nm); dotted lines are spectra collected from the native hydrophobic QDs in organic solvent, and the solid lines designate spectra collected from hydrophilic QDs photoligated with bis(LA)-PEG-OCH_3. The absorption and PL spectra were normalized with respect to the band edge peak and the emission maximum, respectively. (f) UV−vis absorption spectra of 10 nm (hydrodynamic radius) AuNPs dispersed in hydrophobic phase (orange), ligand exchanged with bis(LA)-PEG-OCH_3 (green), and LA-$(PEG\text{-}OCH_3)_2$ (red). The strong absorbance below 350 nm measured for bis(LA)-PEG-OCH_3-AuNPs is due to a stronger contribution from the ligand. The spectra were normalized with respect to the surface plasmon resonance peak at 520 nm.

include the design of ligands with multiple functionalities and the use of versatile and scalable reaction schemes.

Here, we report the design and synthesis of two sets of multicoordinating ligands that are suitable for capping both QDs and AuNPs. The present synthetic scheme starts from L-aspartic acid to develop a versatile platform that allows controllable coupling of one or more lipoic acid (LA) groups, one or more polyethylene glycol (PEG) moieties, along with terminal reactive groups, yielding molecular-scale ligands with various architectures and selective reactivity. We have prepared a series of ligands presenting either one PEG chain appended with two lipoic acid (e.g., bis(LA)-PEG), or two PEG chains attached onto one lipoic acid (e.g., LA-$(PEG)_2$). The chemical structures of the ligands described in this study are shown in Figure 1. This synthetic route provides high reaction yield at each step, and the ligand synthesis can be easily scaled up. We have applied these ligands to cap AuNPs and luminescent QDs. Additionally, these ligands are fully compatible with a mild photoligation strategy to promote the in situ ligand exchange and phase transfer of hydrophobic QDs to buffer media.[59,69,70] The nanocrystals ligated with bis(LA)-PEG exhibit remarkable colloidal stability over a broad range of biological conditions; for instance, AuNPs capped with bis(LA)-PEG show improved resistance to sodium cyanide digestion, as compared to dithiol-capped nanoparticles. Incorporation of acid or amine groups in the ligand coating permits covalent conjugation of a specific

DOI: 10.1021/jacs.5b10359
J. Am. Chem. Soc. 2015, 137, 16084−16097

protein or dye-labeled peptide to the QDs using common bioconjugation strategies. In particular, we show that QDs coupled to transferrin facilitate efficient intracellular uptake of QDs, while QD−peptide conjugation has been confirmed by quantifying the fluorescence resonance energy transfer interactions measured for QD−peptide−dye assemblies.

RESULTS AND DISCUSSION

Ligand Design. One key feature of our design is the use of a single precursor, the amino acid L-aspartic acid, to prepare the various ligands described in this report. The ability to selectively activate one or two groups in the aspartic acid allows one to build up the desired structure, while controlling the nature and number of coordinating groups as well as the number of hydrophilic PEG moieties introduced in the same ligand. Additionally, the various synthetic steps rely mainly on conventional peptide coupling chemistry (e.g., BOC protection and deprotection under acidic conditions along with carbodiimide chemistry). Thus, our design allows the introduction of several reactive groups (e.g., $-N_3$, $-NH_2$, −COOH) in the ligands and provides high reaction yield at each step. Several ligand architectures, including bis(LA)-PEG (higher coordination ligands) and LA-$(PEG)_2$ (ligands with higher PEG branching), have been prepared (see Figure 1). The present route for preparing bis(LA)-appended ligands is simpler than the Michael addition reaction we have previously employed and is more effective for introducing terminal reactive groups in the ligands.[64] Furthermore, comparison between NP coating with either bis(LA)-PEG or LA-$(PEG)_2$ has allowed us to explore the effects of coordination versus steric hindrance on the surface ligand density. For LA-$(PEG)_2$, one can combine terminally inert PEG and PEG-appended with a reactive group within the same ligand by coupling NH_2-PEG-OCH_3 and NH_2-PEG-N_3 sequentially onto the Boc-aspartic acid. A few additional precautions have to be applied, nonetheless. The use of Boc-anhydride as an amine protection eliminates issues of cross coupling, while selective mono coupling is achieved by controlling the molar ratio of DCC (coupling reagent) and Boc-aspartic (e.g., a molar ratio of 1.1:1 was used in the scheme shown in Figure 1A, step (ii)). The use of LA-ethylenediamine permits the introduction of lipoic acid via DCC coupling onto COOH group in the aspartic acid (Figure 1A, step (iii)). To functionalize the bis(LA)-PEG ligands, NH_2-PEG_{1000}-N_3 is substituted for NH_2-PEG_{750}-OCH_3; transformation of the azide to amine and acid follows conventional chemical modifications.[54] The synthesis of LA-$(PEG)_2$ ligands is slightly simpler, as coupling of two PEG moieties could be carried out in the same step as shown in Figure 1C and D. Finally, we should note that the chiral nature of the L-aspartic acid, with its off plane arrangements of the three reactive arms, yields ligands where the anchoring groups and the hydrophilic/reactive functionalities do not lay in the same plane. This offers reduced steric hindrance and may improve the ligand packing on the NP surfaces.

It should be noted that some of the intermediate compounds (precursors), such as compound **4′** and compound **7′**, can be used as capping ligands for QDs or AuNPs. Indeed these two compounds provide two commonly used reactive groups, amine and azide, that can be further modified. For example, compound **4′** can potentially allow the attachment of target small molecules (redox complexes) very close to the NP surface. Similarly, compound **7′** combines both azide and amine on the same ligand, which can permit dual targeting of the NPs with different biomolecules, or transformation of the amine to acid, yielding azide/acid-functionalized NPs.

Ligand Exchange and Optical Characterization of the Nanocrystals. The prepared ligands are compatible with photoligation as a means of promoting in situ cap exchange and phase transfer of TOP/TOPO-QDs to polar and buffer media.[69] This strategy exploits the photochemical transformation of lipoic acid in the presence of UV irradiation (∼330−360 nm) and starts with the oxidized form of the ligands, eliminating the need for chemical reduction of the LA groups prior to phase transfer.[69] Furthermore, this scheme is mild toward sensitive groups such as azide and aldehyde, two functions that are highly desirable in bio-orthogonal chemistry. It is also compatible with other LA-based hydrophilic ligands such as LA-zwitterion.[65,69]

The photoligation was applied to cap exchange a few different size QDs with the new ligands, as shown in Figure 2. The absorption and PL spectra collected from the four sets of QDs before and after phase transfer to DI water were essentially identical, indicating that the photoligation strategy did not alter the photophysical properties of the nanocrystals (Figure 2d−e). Similar observations were collected for QDs photoligated with LA-$(PEG\text{-}OCH_3)_2$ ligands. Phase transfer of AuNPs was more straightforward as it did not require chemical reduction or photoirradiation of the ligand prior to coating of the NPs. The oxidized ligands (i.e., bis(LA)-PEG and LA-$(PEG)_2$) were used; reduction of the dithiolanes upon coordination onto the Au surfaces is expected to take place.[71] Figure 2f shows that the SPR peaks in the absorption spectra collected from dispersions of AuNPs before and after phase transfer are essentially identical, indicating no change in the size or integrity of the nanoparticles after ligand exchange.

Colloidal Stability Tests Applied to QDs and AuNPs. We focused on the colloidal stability of both types of materials phase transferred using bis(LA)-PEG as these ligands are expected to provide stronger binding onto the metal-rich surfaces of the nanocrystals. Tests carried out using LA-$(PEG)_2$ were used as reference. Colloidal stability tests of QDs photoligated with bis(LA)-PEG-OCH_3 were carried out in the presence of added excess NaCl, cell growth media, and acidic and basic pHs; additionally, we probed the long-term stability of dispersions at very low concentrations stored at room temperature and under light exposure. Colloidal stability is most critical for applications in biology where media rich in reducing agents and salts are used, and rather low nanocrystal concentrations are needed for imaging and sensing.[64] The fluorescence images in Figure 3a indicate that QDs photoligated with bis(LA)-PEG-OCH_3 stayed homogeneously dispersed with no sign of aggregation over the pH range 3−14 for at least 6 months of storage at 4 °C (duration of the test). These dispersions also remained stable in the presence of 1 and 2 M NaCl and when dispersed in 50%, 100% cell growth media. Stability tests of these bis(LA)-PEG-OCH_3-QD dispersions at nanomolar concentration were carried by visual examination combined with tracking of the PL emission with storage time. The progression of the fluorescence intensity collected from 50 and 100 nM QD dispersions was tracked over a 6-week period (see Figure 3d). Both dispersions stayed homogeneous and remained fluorescent for 6 weeks (test period), although the PL signal progressively decayed to ∼50% of its initial value. This is promising as compared to data collected for dispersions of QDs capped with monothiol-PEG and even DHLA-PEG ligands, where PL is strongly reduced

DOI: 10.1021/jacs.5b10359
J. Am. Chem. Soc. 2015, 137, 16084−16097

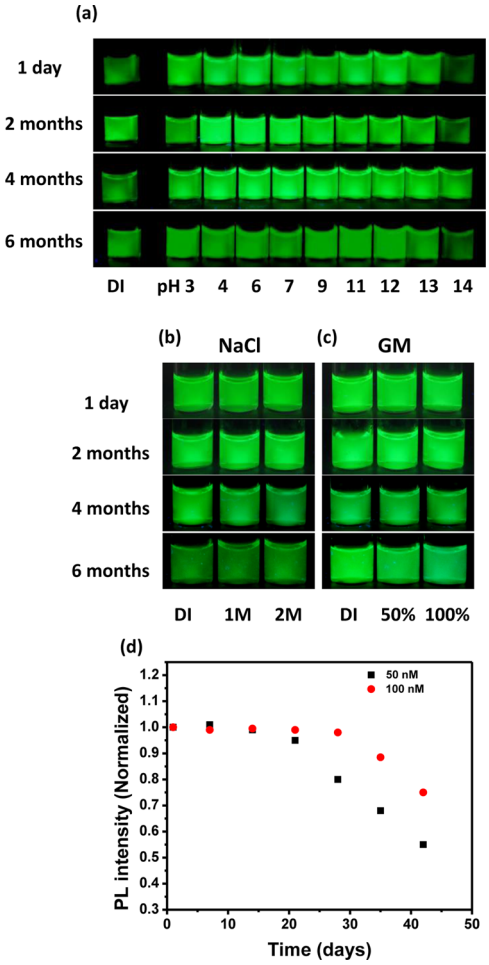

Figure 3. (a–c) Fluorescence images of dispersions of QDs (λ_{em} = 540 nm) photoligated with bis(LA)-PEG-OCH_3 (at 0.5 μM): (a) in 10 mM PBS buffer at different pH values from 3 to 14; (b) in the presence of 1 and 2 M NaCl; (c) in the presence of 50% and 100% RPMI growth media (GM). (d) Plot of PL intensity versus storage time of QDs (λ_{em} = 540 nm) photoligated with bis(LA)-PEG-OCH_3 at 50 and 100 nM. The samples were stored at ambient conditions with exposure to room light.

under similar storage conditions.[45,70] The result is attributed to the higher coordination of the photoligated bis(LA)-PEG ligands onto the QDs.

Similarly, bis(LA)-PEG-OCH_3 was found to provide AuNPs with excellent long-term colloidal stability over the pH range 2–14, in the presence of excess NaCl and in cell growth media for over 1 year of storage under ambient conditions (Figure 4). Additional tests compared the stability of AuNPs ligated with either LA-$(PEG)_2$ or bis(LA)-PEG ligands (lower coordination and larger spatial extension, and vice versa) against NaCN digestion. Cyanide anions (CN^{-1}) are highly reactive toward metal surfaces and can digest AuNP cores, forming $Au(CN)_2^-$ complexes in the medium.[68,72] This results in progressive loss of the plasmonic absorption feature.[68] This test was applied to AuNPs (R_H = 10 nm) ligated with LA-PEG-OCH_3, LA-$(PEG\text{-}OCH_3)_2$, and bis(LA)-PEG-OCH_3, and provided a side-by-side comparison of the effects of coordination, ligand size, and spatial extension of the PEG moieties on the NPs stability to NaCN digestion. Aliquots of 6.2 M NaCN solution (5 μL) were added to dispersions of all three ligated-AuNPs (using final AuNP and NaCN concentrations of 6.3 nM and 62 mM, respectively), and the absorption spectra were collected every 20 min for periods ranging from 1.5 to 10 h. Figure 4d shows that the absorption rapidly decreased for LA-PEG-OCH_3-AuNPs to nearly baseline values after 1.5 h; the dispersion progressed from pinkish-red to completely colorless, indicating the near complete digestion of the AuNP cores. In comparison, a slightly slower loss in the plasmonic absorption (corresponding to a slower digestion) was measured for LA-$(PEG\text{-}OCH_3)_2$-AuNPs, where background level was reached after 3.5 h. The strongest resistance was measured for dispersions of bis(LA)-PEG-OCH_3-AuNPs, where nearly complete digestion of the AuNPs was reached after 10 h (see Figure 4f). We further assessed the rate of decomposition by measuring the time-dependent decrease of the surface plasmon peak at 520 nm and fitting it to a first-order exponential decay function of the form:

$$y = y_0 \times e^{-t/t_D} \quad (1)$$

where t_D designates the decay time and y_0 is the absorbance value at t = 0, as shown in Figure 4g. The decay time (t_D) extracted from fits to the data collected from the various AuNP samples are 56 min for LA-PEG-OCH_3-AuNPs, 75 min for LA-$(PEG\text{-}OCH_3)_2$-AuNPs, and 526 min for bis(LA)-PEG-OCH_3-AuNPs.[68] We found that t_D (bis(LA)-PEG-OCH_3) is ~1 order of magnitude longer than t_D (LA-PEG-OCH_3).

Colloidal Stability against Ligand Desorption. It is understood that coordination of the ligands onto the QDs is not irreversible.[14,41] There is equilibrium between bound and free ligands in the dispersions, with stronger coordination producing lower dissociation constant and vice versa. Phase transfer performed via ligand exchange is usually carried out in the presence of a large excess of the new ligands because the process is driven by mass action. Thus, following ligand exchange dispersions are routinely purified by removing as much as possible the fraction of free solubilized ligands via centrifugal precipitation using a solvent mixture when organic media are used. For dispersions in buffer media, free ligands are removed by applying a few rounds of concentration/dilution using a membrane centrifugal filtration device (with a defined molecular weight cut-off, as described in the Experimental Section). This procedure relies on the ability of centrifugal forces to counterbalance the osmotic pressure in the dispersion (due to a lower chemical potential of the mixture) and extrude the solvent along with solubilized small molecules, including ligands, through the membrane filter. If the procedure is excessively applied, ligand desorption can shift the adsorption/desorption equilibrium between surface-bound and free ligands, resulting in instability buildup and eventually aggregation of the nanoparticles. When using DHLA and DHLA-based ligands for stabilizing QDs, we often apply the above procedure 3–4 times, while finding that stickiness to membrane can take place when more than 5 rounds are applied using ~2000 g (~ 38000 RPM) for ~7–10 min.[71] We tested the colloidal stability of QDs photoligated with bis(LA)-PEG-OCH_3 and AuNPs capped with the same ligand, by extending the rounds of centrifugation/dilution applied to dispersions of both materials. We found that the bis(LA)-PEG-OCH_3 ligands significantly reduced the ligand desorption rate and provided homogeneous and aggregate-free QD dispersions in buffer media even after 8 and 9 rounds of purification. Figure 5 shows that the absorption and emission spectra of QDs were essentially unchanged between the first and eighth rounds. When the test was carried out using AuNPs, additional 10 rounds of membrane centrifugal filtration were

DOI: 10.1021/jacs.5b10359
J. Am. Chem. Soc. 2015, 137, 16084–16097

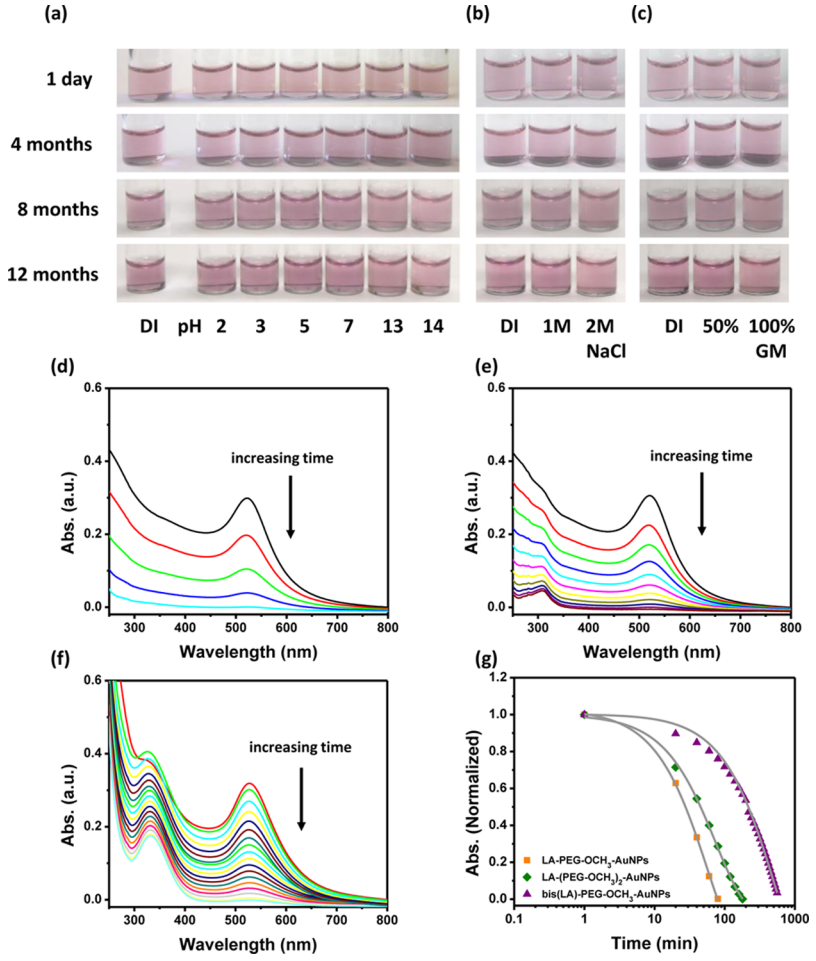

Figure 4. (a–c) White light images of 10 nm AuNPs (hydrodynamic radius) ligand exchanged with bis(LA)-PEG-OCH_3 (1 nM): (a) in 10 mM PBS buffer with pH values ranging from 2 to 14; (b) in the presence of 1 and 2 M NaCl; (c) in the presence of 50% and 100% RPMI growth media (GM). A control dispersion of AuNPs in DI water is also shown. (d–f) Time-progression of the UV–vis absorption spectra of dispersions of AuNPs (6.3 nM) collected in the presence of NaCN (62 mM): (d) LA-PEG-OCH_3-AuNPs; (e) LA-$(PEG\text{-}OCH_3)_2$-AuNPs; (f) bis(LA)-PEG-OCH_3-AuNPs. The spectra shown in (d) and (e) were collected at 20 min intervals, while the spectra shown in (f) were collected at 40 min intervals. The progressive digestion of the AuNPs by added NaCN is reflected by the decrease of the SPR peak with time. The absorption feature at 335 nm (e and f) is attributed to the reformation of lipoic acid after digestion of the AuNP cores. (g) A semilogarithmic plot of time-progression of the SPR measured for AuNPs capped with the three sets of ligands extracted from the data shown in (d)–(f); data were normalized with respect to the value at $t = 0$. The solid lines are fits to eq 1.

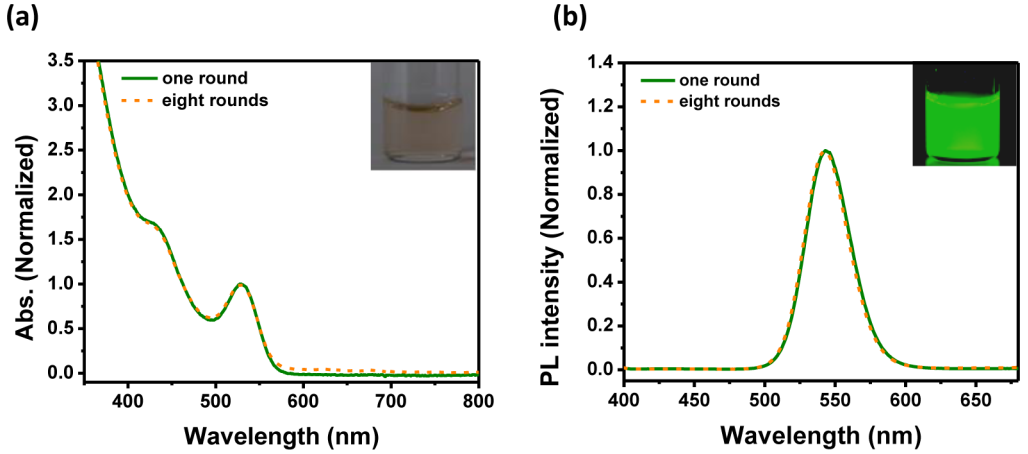

Figure 5. (a) UV–vis absorption and (b) PL spectra of dispersions of bis(LA)-PEG-OCH_3-QDs (λ_{em} = 540 nm) after one (green) and eight rounds (orange) of purification using a centrifugal membrane device as described in the text. The absorption and PL spectra were normalized with respect to the band edge peak and the emission maximum, respectively. The insets show the white light and fluorescence images of the bis(LA)-PEG-OCH_3-QDs after eight rounds of purification and then dispersion in DI water.

DOI: 10.1021/jacs.5b10359
J. Am. Chem. Soc. 2015, 137, 16084–16097

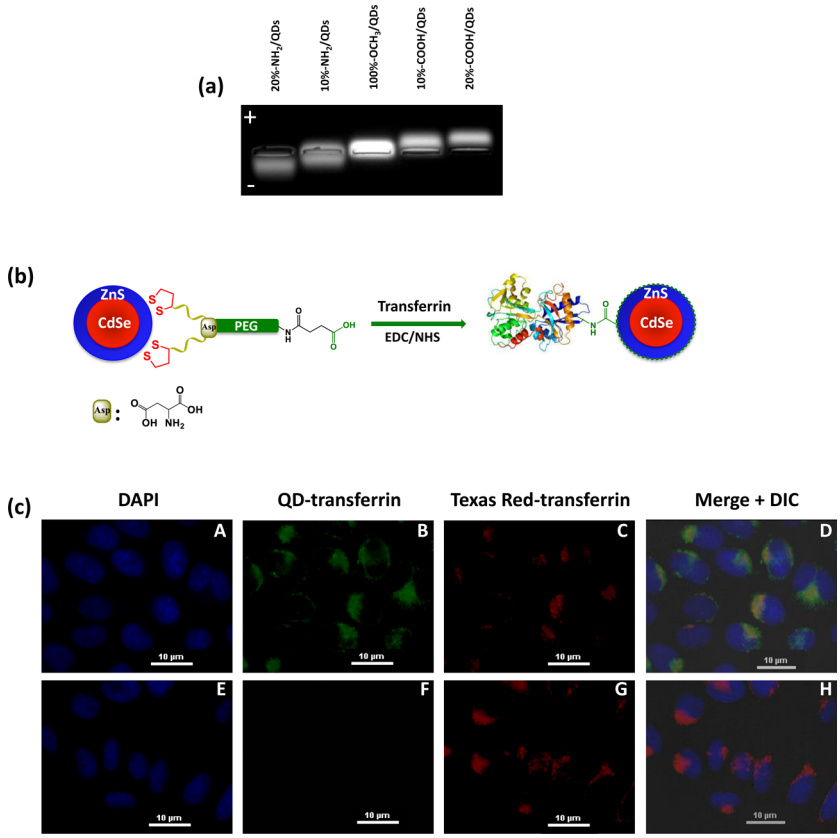

Figure 6. (a) Gel electrophoresis image of QDs photoligated with a mixture of bis(LA)-PEG-NH_2/bis(LA)-PEG-OCH_3 and bis(LA)-PEG-COOH/bis(LA)-PEG-OCH_3 with different molar fractions of reactive ligands; the dispersion of 100% bis(LA)-PEG-OCH_3-QDs was used as control. The intensity difference of the spots is due to the slightly different amount of QD materials used when running the gel. (b) Schematic representation of the coupling between bis(LA)-PEG-COOH-QDs and transferrin via EDC/NHS coupling. (c) Representative epifluorescence images of the QD-transferrin cellular delivery. Hela cells were incubated with green emitting QD-transferrin (λ_{em} = 540 nm, 150 nM) (A–D) and nonconjugated QDs (λ_{em} = 540 nm, 150 nM) (E–H) for 1.5 h. The fluorescence images of cell nuclei counterstained with DAPI, QD-transferrin distribution, endosomes stained with Texas Red, and the merged images for both cases are provided.

applied for LA-PEG-AuNPs and bis(LA)-PEG-AuNPs dispersions following ligand exchange (data not shown). In both cases, the AuNP dispersions stayed homogeneous, with no aggregate buildup. This can be attributed to the strong coordination between thiol/sulfur and surface Au atoms in the AuNP dispersions.

The above results combined are promising and further confirm that higher coordination ligands bind stronger onto the QD surfaces, thus greatly improving the nanocrystal colloidal stability in buffers under several conditions. They clearly demonstrate that higher coordination provides better resistance of AuNPs against sodium cyanide digestion. Our data also show that higher PEG branching (i.e., LA-(PEG-OCH_3)$_2$) yields slightly better protection of the NPs as compared to LA-PEG-OCH_3 ligands, attributed to the denser PEG packing on the nanoparticle surfaces.

Intracellular Delivery of QD-Transferrin Conjugates. Our design can be combined with the use of mixed ligand exchange to prepare QDs that present varying numbers of reactive groups. This can be achieved by introducing (during the ligation step) a controllable fraction of −COOH, $-NH_2$, or $-N_3$-modified ligands along with the inert-terminated ones. The gel electrophoresis image in Figure 6a shows that the gel mobility shift of the QDs depends on the nature and fraction of terminally modified ligands introduced during the phase transfer step.[49] We utilized 540 nm-emitting QDs photoligated with 15% bis(LA)-PEG-COOH to carry out covalent attachment of transferrin to the QDs via EDC/NHS coupling. The reaction targeted available amines on the protein surface. The formed conjugates were further tested for their biological activity by incubating the QD-transferrin conjugates (150 nM) with HeLa cells at 37 °C for 1 h; transferrin is a glycoprotein that binds to specific receptors on the cell surface, promoting its transport inside the cell via receptor-mediated endocytosis.[73] Cells incubated with nonconjugated QDs or with Texas Red-transferrin, respectively, provided negative and positive control experiments. A representative set of epifluorescent images, shown in Figure 6c (panels A–D), indicates that an efficient intracellular uptake of the QD-transferrin conjugates has taken place. The green QD fluorescence was mostly distributed in the perinuclear region of the cells; the nuclei were counterstained with DAPI. Additionally, the fluorescence pattern of the QDs was colocalized with that of Texas Red dye-labeled transferrin, indicating that the nanocrystals were primarily distributed within the endosomal compartments. Conversely, we did not observe any detectable fluorescence signal from the culture incubated with QDs only (control), indicating the absence of nonspecific interactions of the QDs with the cell membranes (see Figure 6c, panels E–H).

QD-Peptide-Cy3 Conjugates and FRET Analysis. Several QD-based sensors using energy or charge transfer interactions (as transduction mechanisms) have been designed

DOI: 10.1021/jacs.5b10359
J. Am. Chem. Soc. 2015, 137, 16084–16097

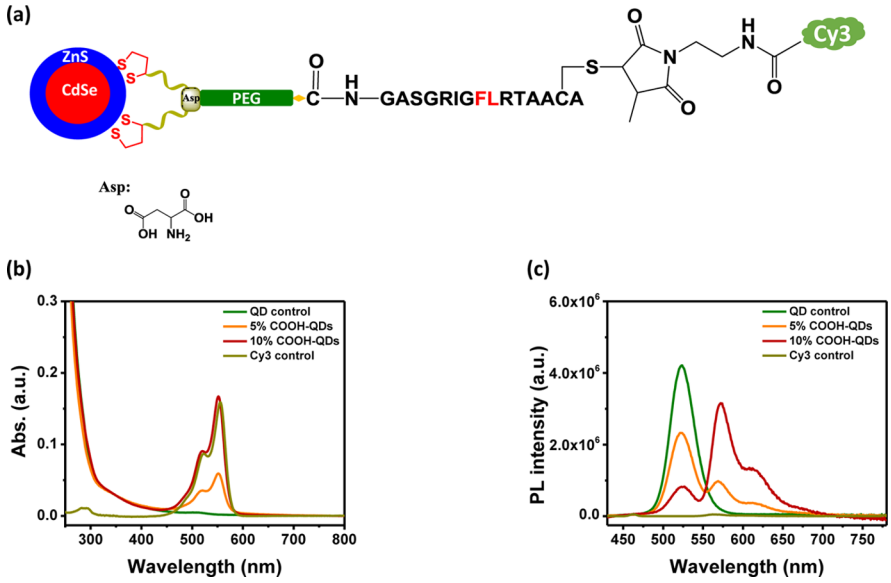

Figure 7. (a) Schematic representation of the coupling of COOH-QDs with Cy3 prelabeled peptide; the sequence of the peptide used is provided. The UV–vis absorption (b) and PL spectra (c) of 5% and 10% COOH-QDs (λ_{em} = 522 nm) conjugated with the peptide-Cy3 via EDC/NHS coupling; QDs alone and dye alone were used as control.

over the past decade using QD-conjugates, to detect properties such as changes in the environment pH, the presence of metal ions, and for monitoring enzymatic activity.[74−77] Designing of QD sensors greatly benefits from the ease of stable surface and ease of coupling with biomolecules of interest.

We have probed the assembly of QD−peptide−dye conjugates formed by coupling the COOH (on bis(LA)-PEG-QDs) with the peptide sequence shown in Figure 7a. The C-terminal cysteine of the peptide was first reacted with maleimide-Cy3, yielding Cy3-labeled peptide, and then the N-terminal amine was further conjugated with COOH-functionalized QDs, via EDC/NHS coupling; two fractions of carboxylic acid-modified QDs (5% and 10%) were used. The composite absorption spectra collected from dispersions of the purified conjugates show contributions from the QDs and Cy3 dye; additionally, the dye contribution to the spectra vary with the fraction of COOH-modified ligands used in the ligand exchange step, indicating that the number of dyes per QD track the fraction of bis(LA)-PEG-COOH ligands used. Figure 7c also shows the emission spectra collected from the same dispersion. There is a progressive loss in QD emission combined with enhancement in the dye PL. Because the samples were excited at 400 nm where direct excitation of the dye is minimal, we attribute the observed fluorescence data to efficient resonance energy transfer between the QDs and bound Cy3, producing strong quenching of the QD signal along with sizable sensitization of the dye fluorescence (see Figure 7c). This is further supported by the pronounced shortening in the QD PL radiative decay time (see Supporting Information). Conversely, the absorption and fluorescence spectra collected from dispersions of Cy3-peptide mixed with methoxy-functionalized-QDs (after purification) show only contribution from the QDs and none from the dye (data not shown). This indicates that no conjugation to the dye-labeled peptide has taken place in the absence of COOH groups on the QD surfaces.

The absorption data were combined with the extinction coefficients of Cy3 (1.5×10^5 M^{-1} cm^{-1} at λ = 552 nm) and green-emitting QDs (3.348×10^5 M^{-1} cm^{-1} at λ = 350 nm), deduced from size and cross-section absorption measurements reported in previous studies,[78,79] to extract an estimate for the number of Cy3 (n) attached to a QD. We measured $n \cong 4$ and $\cong 12$ for conjugates prepared with 5% and 10% COOH-modified QDs, respectively.[79] Similarly, analysis of the deconvoluted fluorescence spectra within the Förster FRET model provided additional estimate for the valence. Assuming a centro-symmetric QD−peptide−dye configuration where acceptors are arrayed around the central donor at a fixed separation distance, the expression for the quenching efficiency, E_n, is given by[80]

$$E_n = \frac{nR_0^{\,6}}{nR_0^{\,6} + r^6} \tag{2}$$

where r represents the separation distance from the donor (QD) to the acceptors and R_0 is the Förster radius corresponding to $E_{n=1}$ = 0.5. Additional details on the FRET analysis are provided in the Supporting Information.

For our system, we used $R_0 \cong 52$ Å, extracted from the experimental spectral overlap and a Q_D value of ~18%. We also used estimates for the QD radius $\cong$ 27 Å (core−shell), the capping layer including a coiled PEG chain in good solvent conditions (end-to-end distance of ~23 Å), a peptide segment of ~11 Å, and the size of the maleimide-dye ~5 Å, to extract a value for the center-to-center separation distance r of $\cong$ 66 Å.[70,81] Using this information and eq 2, we estimated that $n \cong 4$ for 5% COOH-QDs and $\cong$ 11 for 10% COOH-QDs. These values are in reasonable agreement with the values obtained from absorption spectra. The high FRET efficiencies measured for our QD−peptide conjugates prove that our ligand design provides compact QDs and QD-conjugates.

We should note that the peptide structure shown in Figure 7a includes a sequence expected to be specifically recognized and cleaved by the enzyme matrix metalloproteinase (MT1-MMP), an extremely important indicator of cancer in cell cultures and tissue. We will pursue measurements of the kinetics of enzyme digestion of the dye−peptide substrate on the QDs both in solution and in cancer cell lines, and hope to report on those findings in future publications.

DOI: 10.1021/jacs.5b10359
J. Am. Chem. Soc. 2015, 137, 16084−16097

CONCLUSION

Starting from the L-aspartic acid, as a precursor, we synthesized several molecular scale multifunctional PEG-based ligands that present two and four coordinating groups and varying architectures. Ligands prepared and tested include bis(LA)-PEG and LA-$(PEG)_2$. This design exploits the availability of two carboxyl and one amine groups in the chiral L-aspartic acid and combines that with the use of BOC (*tert*-butyloxycarbonyl) protection and carbodiimide chemistries to synthesize several capping ligands with controlled architecture, coordination, and reactivity. The ligands were applied to cap AuNPs and QDs and transfer them to buffer media. The resulting nanoparticles exhibited great long-term colloidal stability over a broad range of conditions. We have also shown that the synthetic strategy permits the attachment of reactive groups including azide, amine, and carboxylic acid, on the same ligand. This allowed conjugation of QDs with biomolecules (transferrin protein and peptide). These were tested for cellular uptake and energy transfer interactions.

QDs or AuNPs coated with these ligands would be greatly useful in sensing applications, based on FRET and charge transfer (CT) interactions including sensing of soluble ions and enzymatic activity. The hydrophilic NPs described here are also promising for intracellular sensing and imaging where colloidal stability at very low concentrations combined with multifunctionality is highly desired. The bis(LA)-PEG and LA-$(PEG)_2$ ligands provide the means to probe the effects of coordination versus steric interactions on the ligand density on inorganic nanocrystals. We should emphasize that amino acids are promising platforms for developing novel organic ligands and the synthetic strategy applied here can be potentially applied to other precursors, such as lysine, to provide ligands for stabilizing other inorganic nanoparticles.

EXPERIMENTAL SECTION

Materials. Poly(ethylene glycol) with molecular weight 600 and 1000 was purchased from Acros Organics (Morris Plains, NJ). Poly(ethylene glycol) methyl ether (molecular weight of 750), L-aspartic acid, lipoic acid (LA), *N*,*N*-dicylohexylcarbodiimide (DCC), 4-(*N*,*N*-dimethylamino)pyridine (DMAP), di-*tert*-butyl dicarbonate (Boc_2O), triphenylphosphine, succinic anhydride, 4 M HCl in dioxane, triethylamine, tetramethylamonium hydroxide (TMAH), and organic solvents (chloroform, methanol, hexane, ethyl acetate, etc.) were purchased from Sigma Chemicals (St. Louis, MO). Phosphate salts used for buffer preparation, NaCl, Na_2CO_3, and Na_2SO_4 were also purchased from Sigma Chemicals. Hydroxybenzotriazole (HOBt·H_2O) was purchased from Alfa Aesar (Ward Hill, MA). Column chromatography purification was performed using silica gel (60 Å, 230−400 mesh, from Bodman Industries, Aston, PA). Sulfo-Cy3 maleimide dye and PD-10 column were purchased from GE Healthcare (Piscataway, NJ). Deuterated solvents used for NMR experiments were purchased from Cambridge Isotope Laboratories Inc. (Andover, MA). The chemicals and solvents were used as received unless otherwise specified. All synthetic reactions described here were carried out under nitrogen atmosphere, unless otherwise specified. Standard nitrogen vacuum manifold technique was used to carry out chemical reactions when needed, and air-sensitive materials were handled in an MBraun Labmaster 130 glovebox (Stratham, NH).

Instrumentation. ^1H NMR spectra were collected using a Bruker SpectroSpin 600 MHz spectrometer (Bruker SpectroSpin, Billerica, MA). A Shimadzu UV−vis absorption spectrophotometer (UV 2450 model, Shimadzu, Columbia, MD) was used to measure the UV−vis absorption spectra from the various dispersions, while the fluorescence spectra were collected on a Fluorolog-3 spectrometer (Jobin Yvon Inc., Edison, NJ) equipped with PMT and CCD detectors. Solvent evaporation (to concentrate or dry samples) was carried out using a lab-scale Buchi rotary evaporator R-215 (New Castle, DE). The photoligation experiments were carried out using a UV photoreactor model LZC-4 V (Luzchem Research Inc., Ottawa, Canada). Gel electrophoresis experiments were performed using a 1% agarose gel. Samples were prepared by diluting dispersions of QDs or QD-conjugates in a TBE buffer (100 mM Tris, 83 mM boric acid, 1 mM EDTA, pH 8.4), then mixing with loading buffer (2.5% ficoll 400, 1.6 mM Tris-HCl, 8.3 mM EDTA, pH 7.4). Aliquots of these dispersions were loaded into the agarose gel and run for 20 min using an applied voltage of 8.0 V/cm. Gel images were captured in the fluorescence mode using a Gel Doc XR+ System.

Ligand Synthesis. The set of ligands prepared in this study, either made of one PEG moiety appended with two lipoic acid anchoring groups (bis(LA)-PEG) or made of two PEG moieties attached onto one lipoic acid (LA-$(PEG)_2$), were all prepared starting from L-aspartic acid as precursor. Our synthetic route also allows easy functionalization of the ligands with various terminal reactive functions such as azide, amine, and acid groups. The poly(ethylene glycol) precursors used for the synthesis, NH_2-PEG_{750}-OCH_3 and NH_2-PEG_{1000}-N_3, were prepared and purified following protocols described in our previous reports.[54,71] These ligands were applied without prereduction of the dithiolane moiety to cap exchange oleylamine-AuNPs. They were, however, combined with the photochemical modification of lipoic acid to achieve in situ ligand exchange and phase transfer of TOP/TOPO-capped QDs. Figure 1 shows the chemical structures along with the synthetic steps used for preparing the various ligands. Below, we detail the synthetic protocols used for preparing these ligands. We should note that PEG_{1000} as well PEG_{600} were used to prepare the terminally-functionalized mono-LA- and bis(LA)-modified ligands. However we found that solubility of the bis(LA)-PEG-capped nanocrystals in aqueous media was better when the longer PEG_{1000} chain was used.

Compound 1 (Boc-Asp). In a 500 mL one-neck round-bottom flask were mixed aspartic acid (Asp, 4 g, ∼30 mmol), 1,4-dioxane (120 mL), and H_2O (60 mL) yielding a heterogeneous solution. An aqueous solution of NaOH (1 M) was added to the mixture with constant stirring until the solution became homogeneous and clear indicating that the aspartic acid was completely dissolved. The solution was cooled using an ice-bath, then di-*tert*-butyl dicarbonate (Boc_2O, 7.2 g, ∼33 mmol) dissolved in 1,4-dioxane (20 mL) was added dropwise. The reaction mixture was then stirred at room temperature overnight. Once the reaction was complete, the solvent was partially evaporated, using a rotary evaporator, to a final volume of ∼30 mL. EtOAc (20 mL) was then added, and the water layer was acidified under ice-cold conditions using an aqueous solution of $KHSO_4$ to pH 2. The solution mixture was transferred to a separatory funnel, and the product was extracted using EtOAc (40 mL, three times). The organic layers were combined and dried over Na_2SO_4. The solvent was evaporated using rotary evaporator, and further vacuum drying was applied overnight to yield the compound as a white solid (∼6 g); reaction yield ∼85%.

^1H NMR (600 MHz, DMSO-d_6): δ 1.38 (s, 9H), 2.51−2.55 (m, 1H), 2.65−2.69 (m, 1H), 4.24−4.28 (m, 1H), 7.05−7.07 (d, 1H, J = 12 Hz), 12.5 (s, 2H).

Compound 2 (Boc-Asp-PEG-OCH_3). Boc-Asp, compound **1** (3.1 g, 13.3 mmol), was dissolved in EtOAc (30 mL) in a 100 mL two-neck round-bottom flask equipped with a magnetic stirring bar. The solution was purged with N_2 and cooled to ∼0 °C using an ice bath, and then a solution of DCC (3.01 g, 14.6 mmol) in EtOAc (30 mL) was added dropwise through an additional funnel over ∼20 min. Once the addition was complete, the mixture was gradually warmed to room temperature and continuously stirred for another 4 h. The white solid byproduct was first removed using a filter paper, and the solvent was evaporated to provide the DCC activated Boc-aspartic acid compound as a white solid. This compound was mixed with NH_2-PEG_{750}-OCH_3 (14.7 g, 20 mmol) and THF (100 mL) in a 250 mL three-neck round-bottom flask, and the solution was refluxed at 66 °C overnight. The reaction mixture was cooled to room temperature, filtered through a filter paper, and chromatographed on a silica column (230−400

DOI: 10.1021/jacs.5b10359
J. Am. Chem. Soc. 2015, 137, 16084−16097

mesh). A one round elution with $CHCl_3$ was first applied to remove impurities, and the product was collected using a mixture of 40:1 (v/v) $CHCl_3$:MeOH as the eluent. After evaporating the solvent, a light yellowish oil was collected (~11 g); reaction yield ~90%. We should note that the mono coupling of NH_2-PEG-OCH_3 and NH_2-PEG-N_3 onto Boc-aspartic acid yields a mixture of two isomers (one is from amine coupling to the α-carboxylic acid and the other is from amine coupling to the β-carboxylic acid); these isomers are eluted together from the gel column, because they have similar polarity. The final products were also collected as isomer mixtures and directly applied for the attachment to LA-ethylenediamine when synthesizing compound **3** and compound **6**. In the synthesis scheme detailed above, only one representative isomer is shown.

^{1}H NMR (600 MHz, $CDCl_3$): δ 1.39 (s, 9H), 2.56−2.60 (m, 1H), 2.91−2.95 (m, 1H), 3.33 (s, 3H), 3.49−3.51 (m, 3H), 3.59−3.60 (m, 64H), 4.43−4.47 (m, 1H), 5.75 (br, 1H), 6.97 (br, 1H).

Compound 3 (Boc-Asp-LA-PEG-OCH_3). In a round-bottom flask, compound **2** (7.1 g, 7.5 mmol) was mixed with THF (50 mL) and cooled under ice-cold conditions. A mixture of DCC (2 g, 9.7 mmol) and HOBt·H_2O (1.5 g, 9.8 mmol) dissolved in THF (15 mL) was added to the reaction flask dropwise under N_2 atmosphere with constant stirring. After the addition was complete, the solution was gradually warmed to room temperature and stirred for 1 h. LA-ethylenediamine (2.8 g, 11.3 mmol) dispersed in $CHCl_3$ (5 mL) was added dropwise via a syringe; LA-ethylenediamine was presynthesized following previous literature.[82] The reaction mixture was left stirring at room temperature for 2 days, then filtered through a filter paper to remove the white solid byproduct. The compound was then purified on a silica gel column in two steps: impurities were first removed by elution with $CHCl_3$. The compound then was eluted using 30:1 (vol:vol) $CHCl_3$:MeOH solvent mixture. Following evaporation of the solvent, the product was collected as a yellow oil (~6.7 g); reaction yield ~76%.

^{1}H NMR (600 MHz, $CDCl_3$): δ 1.42−1.48 (m, 11H), 1.61−1.73 (m, 4H), 1.87−1.93 (m, 1H), 2.21−2.23 (t, 2H, J = 6 Hz), 2.42−2.48 (m, 1H), 2.57−2.60 (m, 1H), 2.71−2.74 (m, 1H), 3.08−3.12 (m, 1H), 3.14−3.18 (m, 1H), 3.37 (s, 3H), 3.39−3.45 (m, 4H), 3.52−3.55 (m, 5H), 3.63 (m, 65H), 4.45−4.49 (m, 1H), 6.20 (br, 1H), 6.91 (br, 1H), 6.99 (br, 1H).

Compound 4 (Bis(LA)-PEG-OCH_3). In a round-bottom flask 4 M HCl in 1,4-dioxane (15 mL) was added to compound **3** (6.7 g, 5.7 mmol) under ice-cold conditions and left stirring for 4 h at room temperature. The solvent was evaporated using rotary evaporator followed by dispersion in H_2O (70 mL). This aqueous solution was transferred to a separation funnel and washed with diethyl ether (50 mL, two times). The aqueous layer was collected, basified using saturated Na_2CO_3 to ~pH 9, and the compound was extracted using $CHCl_3$ (50 mL, three times). The solvent was finally evaporated to obtain the Boc-deprotected product (compound **4′**, 5.5 g, yield ~90%). This Boc-deprotected compound (5.5 g, 5.1 mmol) was mixed with LA (1.6 g, 7.8 mmol) and DMAP (0.2 g, 1.6 mmol) in $CHCl_3$ (50 mL), and the mixture was cooled to ~0 °C under ice-cold conditions. DCC (1.6 g, 7.8 mmol) dissolved in $CHCl_3$ (15 mL) was added dropwise, and then the reaction was stirred for 2 days at room temperature. The white solid byproduct was removed by filtration, and the chloroform layer was further washed with saturated sodium carbonate solution (30 mL, two times) to remove excess unreacted lipoic acid. The solution was concentrated and purified on a silica gel column using a 30:1 (vol:vol) $CHCl_3$:MeOH as eluent. After solvent evaporation, the product was finally collected as a yellow solid (~4.5 g); reaction yield ~70%.

^{1}H NMR (600 MHz, $CDCl_3$): δ 1.46−1.51 (m, 4H), 1.65−1.73 (m, 8H), 1.9−1.95 (m, 2H), 2.22−2.24 (t, 2H, J = 6 Hz), 2.26−2.28 (t, 2H, J = 6 Hz), 2.45−2.85 (m, 2H), 2.53−2.57 (m, 1H), 2.67−2.7 (m, 1H), 3.11−3.18 (m, 2H), 3.18−3.22 (m, 2H), 3.39 (s, 3H), 3.44−3.47 (m, 4H), 3.55−3.59 (m, 8H), 3.65 (m, 65H), 4.74−4.77 (m, 1H), 6.80 (br, 1H), 6.90 (br, 1H), 7.40 (br,1H).

Compound 5 (Boc-Asp-PEG-N_3). Boc-aspartic acid (compound **1**, 2.1 g, 9.0 mmol) was dissolved in EtOAc (30 mL) using a 100 mL two-neck round-bottom flask equipped with a magnetic stirring bar. The solution was cooled using an ice bath, purged with N_2, and DCC (2.04 g, 9.9 mmol) dissolved in EtOAc (20 mL) was added dropwise. The reaction was gradually warmed to room temperature and left stirring for 4 h. The white solid byproduct was first removed using a filter paper, followed by solvent removal using a rotary evaporator. The obtained white powder was mixed with NH_2-PEG_{1000}-N_3 (14 g, 13.5 mmol, dissolved in 100 mL of THF) and refluxed at 66 °C overnight. The product mixture was cooled to room temperature, filtered through filter paper, dried over Na_2SO_4, concentrated using rotary evaporator, and chromatographed on a silica gel column. The pure product was collected using a solvent mixture of 20:1 (vol:vol) $CHCl_3$:MeOH for elution. A light yellow oil was collected after evaporating the solvent (~10 g); reaction yield ~90%.

^{1}H NMR (600 MHz, $CDCl_3$): δ 1.38 (s, 9H), 2.62−2.66 (m, 1H), 2.82−2.94 (m, 1H), 3.33−3.34 (m, 5H), 3.47−3.5 (m, 5H), 3.59 (m, 90H), 4.39−4.43 (m, 1H), 5.56 (br, 1H), 6.80 (br, 1H).

Compound 6 (Boc-Asp-LA-PEG-N_3). Compound **5** (5 g, 4 mmol) and THF (40 mL) were mixed in a 100 mL two-neck round-bottom flask equipped with a magnetic stirring bar. A solution mixture of DCC (1.1 g, 5.3 mmol), HOBt·H_2O (0.8 g, 5.2 mmol), and THF (10 mL) was added to the flask dropwise under ice-cold conditions. The mixture was stirred at room temperature for 1 h, and then LA-ethylenediamine (1.48 g, 6 mmol) dissolved in $CHCl_3$ (5 mL) was subsequently added dropwise. The reaction mixture was left stirring at room temperature and under N_2 atmosphere for 2 days. Once the reaction was completed, the mixture was filtered using a filter paper (to remove the white solid byproduct), and the solution was concentrated under vacuum using a rotary evaporator, then purified on a silica gel column using a mixture of 30:1 (vol:vol) $CHCl_3$:MeOH as eluent. The product was collected as a yellow oil (~4.7 g); reaction yield ~79%.

^{1}H NMR (600 MHz, $CDCl_3$): δ 1.42−1.46 (m, 11H), 1.63−1.69 (m, 4H), 1.86−1.92 (m, 1H), 2.29−2.31 (t, 2H, J = 6 Hz), 2.42−2.47 (m, 1H), 2.71−2.74 (m, 1H), 2.75−2.78 (m, 1H), 3.07−3.11 (m, 1H), 3.14−3.18 (m, 1H), 3.37−3.4 (m, 6H), 3.54−3.55 (m, 4H), 3.62 (m, 90H), 4.52−4.55 (m, 1H).

Compound 7 (Bis(LA)-PEG-N_3). Deprotection of the BOC group was applied to compound **6**: 4 M HCl in 1,4-dioxane (15 mL) was added to 4 g (2.7 mmol) of compound **6**, and the mixture was stirred for 4 h at room temperature. The purification was carried out following the same procedure used in the synthesis of compound 4, as detailed above. This deprotected product (compound **7′**, 3 g, 2.17 mmol), LA (0.67 g, 3.25 mmol), and DMAP (0.08 g, 0.66 mmol) were dissolved in $CHCl_3$ (20 mL) followed by dropwise addition of a DCC solution in $CHCl_3$ (0.67 g, 3.25 mmol, 10 mL) under ice-cold conditions. The reaction mixture was purged with N_2 and stirred for 2 days at room temperature. A white solid byproduct was removed by filtration, the $CHCl_3$ layer was washed with saturated Na_2CO_3 solution (15 mL, two times), and then the solution mixture was purified on a silica gel column using 30:1 (vol:vol) $CHCl_3$:MeOH mixture as the eluent to obtain compound 7 as a yellow solid (~2.3 g); reaction yield ~67%.

^{1}H NMR (600 MHz, $CDCl_3$): δ 1.42−1.47 (m, 4H), 1.64−1.69 (m, 8H), 1.86−1.92 (m, 2H), 2.21−2.23 (t, 2H, J = 6 Hz), 2.24−2.26 (t, 2H, J = 6 Hz), 2.42−2.48 (m, 2H), 2.65−2.69 (m, 1H), 2.78−2.82 (m, 1H), 3.08−3.12 (m, 2H), 3.15−3.19 (m, 2H), 3.4−3.43 (m, 5H), 3.51−3.56 (m, 6H), 3.63 (m, 90H), 4.70−4.75 (m, 1H), 6.90 (br, 1H), 7.10 (br, 1H), 7.40 (br, 1H).

Compound 8 (Bis(LA)-PEG-NH_2). Compound **7** (2.9 g, 1.86 mmol) was dissolved in THF (50 mL) at room temperature with constant stirring; a slight heating may be required to ensure that the compound is completely dissolved. Triphenylphosphine (0.73 g, 2.8 mmol) was added (at room temperature), and the reaction mixture was stirred for 40 min under N_2, followed by addition of H_2O (0.33 mL, 18.3 mmol); the reaction mixture was further left stirring overnight. Once the reaction was complete, the solvent was evaporated using a rotary evaporator, and then EtOAc was added to the residue and stirred with slight heating (~60 °C) to dissolve the compound. The solution was transferred to a separatory funnel, to which 1 M HCl (50 mL) was added. The organic layer was removed, and the aqueous

DOI: 10.1021/jacs.5b10359
J. Am. Chem. Soc. 2015, 137, 16084−16097

layer was further washed with EtOAc (40 mL, 1 time) to remove the remaining impurities. Saturated Na_2CO_3 solution was added to the aqueous layer to basify the solution (~pH 9). The final product was extracted with $CHCl_3$ (50 mL, three times), dried over Na_2SO_4, and collected after evaporating the solvent as a yellow oil (~1.8 g); reaction yield ~62%.

^{1}H NMR (600 MHz, $CDCl_3$): δ 1.42−1.47 (m, 4H), 1.63−1.68 (m, 8H), 1.85−1.89 (m, 2H), 2.18−2.20 (t, 2H, J = 6 Hz), 2.22−2.24 (t, 2H, J = 6 Hz), 2.42−2.48 (m, 2H), 2.53−2.56 (m, 1H), 2.75−2.79 (m, 1H), 2.83−2.87 (t, 2H, J = 6 Hz), 3.08−3.12 (m, 2H), 3.15−3.19 (m, 2H), 3.33−3.39 (m, 6H), 3.51−3.56 (m, 6H), 3.63 (m, 90 H), 4.71−4.75 (m, 1H).

Compound 9 (Bis(LA)-PEG-COOH). Bis(LA)-PEG-NH_2 (compound **8**, 1 g, 0.65 mmol), succinic anhydride (0.13 g, 1.3 mmol), triethylamine (0.23 mL, 1.69 mmol), and $CHCl_3$ (20 mL) were mixed in a 100 mL one-neck round-bottom flask. The mixture was stirred at room temperature overnight under N_2 atmosphere. The solvent was removed under vacuum, and 1 M HCl (20 mL) was added to the residue. The product was further extracted using $CHCl_3$ (30 mL, three times). The organic layers were combined, dried over Na_2SO_4, filtered through a filter paper, and the solvent was evaporated, yielding the final product (compound **9**) as a yellow oil (~0.63 g); reaction yield ~60%.

^{1}H NMR (600 MHz, $CDCl_3$): δ 1.4−1.46 (m, 4H), 1.64−1.7 (m, 8H), 1.88−1.93 (m, 2H), 2.24−2.29 (m, 4H), 2.44−2.49 (m, 2H), 2.54−2.56 (m, 1H), 2.61−2.65 (m, 4H), 2.74−2.78 (m, 1H), 3.09−3.12 (m, 2H), 3.14−3.19 (m, 2H), 3.34−3.4 (m, 6H), 3.50−3.55 (m, 6H), 3.64 (m, 90 H), 4.72−4.75 (m, 1H).

Compound 10 (Boc-Asp-(PEG-OCH_3)$_2$). Compound **1** (1 g, 4.29 mmol), NH_2-PEG_{750}-OCH_3 (7.6 g, 10.34 mmol), and DMF (20 mL) were mixed in a 100 mL two-neck round-bottom flask equipped with a magnetic stir bar. The solution was stirred at room temperature until all of the solid materials were fully dissolved. DCC (1.9 g, 9.22 mmol) and HOBt·H_2O (1.41 g, 9.22 mmol) dissolved in DMF (10 mL) were further added dropwise using a syringe under ice-cold conditions. Once the addition was complete, the mixture solution was warmed to room temperature and left stirring for 2 days under N_2 atmosphere. The reaction mixture was filtered through a filter paper (to remove the white solid byproduct), and then $CHCl_3$ (40 mL) was added. This solution was further washed with 1 M HCl (20 mL, 1 time) and saturated Na_2CO_3 (20 mL, 1 time), dried by adding Na_2SO_4, and the solvent was evaporated using a rotary evaporator. The residue was chromatographed on a silica gel column with 25:1 (vol:vol) $CHCl_3$:MeOH mixture as eluent, yielding the product as a yellow oil (~6.2 g); reaction yield ~86%.

^{1}H NMR (600 MHz, $CDCl_3$): δ 1.39 (s, 9H), 2.51−2.54 (m, 1H), 2.8−2.83 (m, 1H), 3.33 (s, 6H), 3.4−3.42 (m, 4H), 3.49−3.59 (m, 9H), 3.60 (m, 140H), 4.39 (m, 1H), 6.14 (br, 1H), 6.65 (br, 1H), 7.14 (br, 1H).

Compound 11 (LA-(PEG-OCH_3)$_2$). The deprotection of compound **10** and purification of the product were carried out following the same procedure as detailed above for compound **7**. The deprotected compound **10** (3 g, 1.91 mmol) was mixed with LA (0.47 g, 2.28 mmol) and DMF (15 mL) in a 100 mL two-neck round-bottom flask equipped with a magnetic stirring bar. In a separate vial, a solution of DCC (0.47 g, 2.28 mmol) and HOBt·H_2O (0.35 g, 2.28 mmol) in DMF (5 mL) was added dropwise to the reaction solution under ice-cold conditions with constant stirring. The reaction solution was gradually warmed to room temperature and left stirring for another 2 days to ensure the completeness of the reaction. After the white solid byproduct was filtered off, the solution was washed with saturated Na_2CO_3 (10 mL, two times), dried over Na_2SO_4, and concentrated using a rotary evaporator. The crude product was further purified over silica gel chromatography using 20:1 (vol:vol) $CHCl_3$:MeOH mixture as eluent to provide a yellow oil paste (~2.5 g); reaction yield ~74%.

^{1}H NMR (600 MHz, $CDCl_3$): δ 1.40−1.52 (m, 2H), 1.62−1.72 (m, 4H), 1.87−1.93 (m, 1H), 2.24−2.26 (t, 2H, J = 6 Hz), 2.43−2.48 (m, 1H), 2.53−2.57 (m, 1H), 2.81−2.85 (m, 1H), 3.08−3.13 (m, 1H), 3.15−2.29 (m, 1H), 3.37 (s, 6H), 3.42−3.46 (m, 5H), 3.52−3.56 (m, 9H), 3.63 (m, 120H), 4.70−4.72 (m, 1H), 7.05 (br, 1H), 7.34 (br, 1H), 7.46 (br, 1H).

Compound 12 (Boc-Asp-(PEG-N_3)$_2$). Boc-aspartic acid (compound **1**, 1.0 g, 4.29 mmol), NH_2-PEG_{1000}-N_3 (10.4 g, 10.27 mmol), and DMF (20 mL) were added to a 100 mL two-neck round-bottom flask containing a magnetic stir bar. The mixture was stirred until a homogeneous solution was formed. A solution of DCC (1.95 g, 9.46 mmol) and HOBt·H_2O (1.45 g, 9.46 mmol) in DMF (5 mL) was added to the reaction mixture dropwise under ice-cold conditions. Once the addition was complete, the reaction solution was gradually warmed to room temperature and left stirring for 2 days. A white solid byproduct was filtered off using a filter paper, and the solvent was evaporated under vacuum. The residue was purified over silica gel column using 20:1 (vol:vol) $CHCl_3$:MeOH mixture as eluent, yielding the product as a yellow oil (~6.2 g); reaction yield ~65%.

^{1}H NMR (600 MHz, $CDCl_3$): δ 1.43 (s, 9H), 2.50−2.53 (m, 1H), 2.83−2.87 (m, 1H), 3.36−3.40 (m, 6H), 2.50−2.53 (m, 5H), 3.63 (m, 175H), 4.40−4.44 (m, 1H), 6.14 (br, 1H), 6.67 (br, 1H), 7.13 (br, 1H).

Compound 13 (LA-(PEG-N_3)$_2$). Compound **12** was deprotected and purified following the same procedure as described above. The deprotected compound **12** (3 g, 1.41 mmol), LA (0.35 g, 1.7 mmol), and DMF (10 mL) were mixed in a 100 mL two-neck round-bottom flask. The solution was stirred until becoming homogeneous, then cooled to ~0 °C using an ice bath. In a separate vial, DCC (0.32 g, 1.55 mmol) and HOBt·H_2O (0.24 g, 1.55 mmol) were dissolved in DMF (5 mL), and then added to the above reaction mixture under N_2 atmosphere. The reaction solution was warmed to room temperature and further stirred for 2 days. The byproduct (as a white solid) was filtered off using a filter paper, and the residue was purified using silica gel chromatography with a 20:1 (vol:vol) $CHCl_3$:MeOH mixture as eluent. The product was obtained as a yellow oil (~2.3 g); reaction yield ~70%.

^{1}H NMR (600 MHz, $CDCl_3$): δ 1.38−1.46 (m, 2H), 1.62−1.67 (m, 4H), 1.96−1.92 (m, 1H), 2.21−2.23 (t, 2H, J = 6 Hz), 2.41−2.46 (m, 1H), 2.62−2.65 (m, 1H), 2.87−2.91 (m, 1H), 3.05−3.09 (m, 1H), 3.12−3.16 (m, 1H), 3.38−3.41 (m, 6H), 3.52−3.55 (m, 6H), 3.62 (m, 175H), 4.73−4.76 (m, 1H), 6.81−6.89 (br, 2H)

Compound 14 (LA-(PEG-NH_2)$_2$). Compound **13** (2 g, 0.87 mmol) was dissolved in THF (40 mL) in a 100 mL one-neck round-bottom flask equipped with a magnetic stirring bar, followed by the addition of triphenylphosphine (0.68 g, 2.6 mmol). The solution was stirred at room temperature under N_2 atmosphere for 30 min, and then H_2O (0.31 g, 17.3 mmol) was added. The reaction mixture was further stirred at room temperature overnight and purified following the same steps as described for preparing bis(LA)-PEG-NH_2 (compound **8**). The product was collected as a yellow oil (~1.2 g); reaction yield ~60%.

^{1}H NMR (600 MHz, $CDCl_3$): δ 1.4−1.45 (m, 2H), 1.59−1.65 (m, 4H), 1.85−1.89 (m, 1H), 2.1−2.3 (t, 2H, J = 6 Hz), 2.39−2.44 (m, 1H), 2.67−2.73 (m, 1H), 2.83−2.85 (t, 4H, J = 6 Hz), 2.84−2.87 (m, 1H), 3.04−3.08 (m, 1H), 3.11−3.15 (m, 1H), 3.37−3.4 (m, 3H), 3.48−3.52 (m, 10H), 3.62 (m, 175H), 4.43−4.46 (m, 1H).

Compound 15 (LA-(PEG-COOH)$_2$). Compound **14** (1 g, 0.44 mmol), succinic anhydride (0.09 g, 0.88 mmol), triethylamine (0.16 mL, 1.15 mmol), and $CHCl_3$ (15 mL) were mixed in a 100 mL one-neck round-bottom flask equipped with a magnetic stirring bar. The reaction was stirred at room temperature overnight under N_2, and then the solvent was evaporated using a rotary evaporator. The residue was dissolved in 1 M HCl (20 mL), and the product was extracted using $CHCl_3$ (40 mL, three times). After drying over Na_2SO_4 and evaporating the organic solvent, compound **15** was obtained as a yellow oil (~0.6 g); reaction yield ~60%.

^{1}H NMR (600 MHz, $CDCl_3$): δ 1.39−1.46 (m, 2H), 1.60−1.66 (m, 4H), 1.86−1.90 (m, 1H), 2.19−2.21 (t, 2H, J = 6 Hz), 2.30−2.46 (m, 1H), 2.60−2.66 (m, 8H), 2.70−2.74 (m, 1H), 2.84−2.88 (m, 1H), 3.25−3.09 (m, 1H), 3.11−2.16 (m, 1H), 3.38−3.41 (m, 6H), 3.50−3.55 (m, 6H), 3.63 (m, 180 H), 4.70−4.74 (m, 1H).

Quantum Dot Synthesis. CdSe−ZnS core−shell QDs with different core sizes were synthesized by reacting organometallic

DOI: 10.1021/jacs.5b10359
J. Am. Chem. Soc. 2015, 137, 16084−16097

precursors (e.g., cadmium acetylacetonate and trioctylphosphine selenium) in hot coordinating solvent mixture made of alkylphosphines, alkyphosphine-carboxyl, and alkylamine.[32,83] As-prepared the QD surfaces were primarily capped with TOP/TOPO ligands, making them highly hydrophobic in nature. Ligand exchange with lipoic acid-modified ligands (described above) were applied to promote their transfer to water media and render them biocompatible.[45]

Photoligation of QDs with LA-Modified Ligands. The phase transfer of the QDs relied on the in situ photochemical transformation of the various LA-modified ligands. We briefly describe the procedure applied to cap the QDs with bis(LA)-PEG-OCH_3 and LA-(PEG-OCH_3)$_2$ (compound **4** and compound **11**) and transfer them to aqueous media. A stock dispersion of TOP/TOPO-capped CdSe-ZnS quantum dots (8 μM, 163 μL) in toluene/hexane mixture was precipitated using ethanol. The turbid mixture was centrifuged at 1900 *g* for 15 min, the supernatant was discarded, and the solid pellet was redispersed in hexane (500 μL). In a separate scintillation vial, bis(LA)-PEG-OCH_3 (68 mg) or LA-(PEG-OCH_3)$_2$ (95 mg) was dissolved in MeOH (500 μL) mixed with a catalytic amount of tetramethylammonium hydroxide (TMAH). The contents of the vials were combined in one vial containing a magnetic stir bar. The vial atmosphere was switched to N_2, then placed inside a UV reactor (Luzchem Research Inc., Ottawa, Canada). The reaction mixture was irradiated with UV light (λ_{irr} peak centered at 350 nm, at a power of 4.5 mW/cm^2) for 30−40 min with continuous stirring. A complete transfer of the QDs from hexane layer to the bottom methanol layer occurred, indicating that ligand exchange of the native TOP/TOPO with the bis(LA)-PEG-OCH_3 or LA-(PEG-OCH_3)$_2$ has indeed taken place. The solvents were evaporated under vacuum, then a solvent mixture (made of 1:1:10 in volume MeOH:$CHCl_3$:C_6H_{14}) was added followed by centrifugation at 1900 *g* for 6 min. The top solvent layer was decanted, and the precipitate was mildly dried under vacuum. The resulting QD pellet was readily dispersed in DI water. The water dispersions of QDs were further purified by applying three rounds of concentration dilution using a centrifugal membrane filtration device with a 50k Da molecular weight cut-off (Amicon Ultra), to remove the free unbound ligands. The same protocol can be applied to prepare QDs that are functionalized with reactive groups such as $-N_3$, $-NH_2$, and −COOH. Here, we simply mix a small fraction of bis(LA)-PEG-N_3, bis(LA)-PEG-NH_2, or bis(LA)-PEG-COOH with the inert bis(LA)-PEG-OCH_3 ligands and follow the steps described above. Similarly, hydrophilic and reactive QDs were prepared using a mixture of LA-(PEG-OCH_3)$_2$ and $-N_3$, $-NH_2$, and −COOH-appended ligands, following the same steps. Note: The dissolution of bis(LA)-PEG-OCH_3 ligands in water requires slight heating and continuous stirring. However, once the disulfide ring is opened followed by ligation with QDs, the obtained nanoparticles are readily dispersed in DI water.

Ligand Exchange on AuNPs. Hydrophobic oleylamine-stabilized AuNPs with a hydrodynamic radius of 10 nm were prepared following a previously detailed synthetic scheme and stored in hexane.[84] Cap exchange of these AuNPs with bis(LA)-PEG-OCH_3 and LA-(PEG-OCH_3)$_2$ was carried out following the same protocol. Here, we briefly describe the cap exchange with bis(LA)-PEG-OCH_3 ligands using either two-phase or one-phase configuration. 1) Two-phase configuration: A stock dispersion of oleylamine-AuNPs (30 nM, 100 μL) in hexane was further diluted with hexane to a total volume of 500 μL. Bis(LA)-PEG-OCH_3 (20 mg) dissolved in MeOH (500 μL) was added to the above dispersion of AuNPs in hexane, and the mixture was left stirring at room temperature overnight. This produces a phase transfer of the AuNPs from the top hexane layer to the bottom methanol layer, indicating that oleylamine has been replaced by bis(LA)-PEG-OCH_3 ligands. The procedure is also expected to induce a reduction of LA to DHLA.[49] The bis(LA)-PEG-OCH_3-AuNPs were purified and dispersed in DI water, by first evaporating the solvent(s), redispersion in a solvent mixture, and centrifugation, using the same conditions as done above for the QDs. Finally, 2−3 rounds of centrifugation using a membrane filtration device (Amicon Ultra, 50 kDa) were used to remove the remaining unbound ligands. 2) Single phase configuration. We used THF as the solvent. Briefly, starting with oleylamine-AuNPs (30 nM, 100 μL) in hexane, the solvent was evaporated under vacuum, and then bis(LA)-PEG-OCH_3 (20 mg) in THF (500 μL) was added forming a homogeneous phase. The solution was stirred at room temperature overnight, and then THF was evaporated under vacuum. To the dry NPs was added a solvent mixture of MeOH:$CHCl_3$:C_6H_{14}, similar to that used above for the QDs, yielding a turbid sample. Following centrifugation, the solvent was decanted, and the sample was gently dried. The resulting precipitate was readily dispersed in water. Then, 2−3 rounds of centrifugation using a membrane filtration device (Amicon Ultra, 50 kDa) were used to purify the AuNPs from excess unbound ligands and solubilized organics.

Conjugation of QDs to Transferrin via EDC Coupling. The QDs (12.5 μM, 40 μL) photoligated with a mixture of bis(LA)-PEG-OCH_3 and bis(LA)-PEG-COOH (85:15 in molar ratio), EDC (52 mM in DI water, 14.4 μL), and NHS (87 mM in DI water, 17.3 μL) were mixed with 178.3 μL of 10 mM phosphate buffer (PB, pH 6.5) in a scintillation vial. The vial was wrapped with aluminum foil, and the mixture was stirred at room temperature for 1 h. Next, 4 mL of 10 mM PB (pH 8.7) was added and the content was subsequently transferred to a membrane filtration device (Amicon Ultra, 50 kDa); then one round of concentration/dilution was applied to remove excess EDC. The sample was concentrated to a final volume of ∼100 μL, and then NHS (87 mM in DI water, 9 μL), transferrin (2.4 mg), and 10 mM PB (pH 8.7) were added; the total volume of the reaction was maintained at 400 μL. The mixture was left to react at room temperature for 5 h with constant stirring, then loaded onto a PD-10 desalting column (GE Healthcare) to remove unreacted transferrin and excess coupling reagents. The conjugates were characterized using absorption spectroscopy before testing them in cellular uptake measurements. The experimental details on the cell uptake and fluorescence imaging are provided in the Supporting Information.

Conjugation of QDs with Peptide (A42). QDs photoligated with 5% and 10% bis(LA)-PEG-COOH were conjugated to a peptide with the sequence of GASGRIGFLRTAACA MW ≈ (1449.4 g/mol). This peptide has a C-terminal cysteine (C) at one end, which was coupled to a maleimide-functionalized dye, and a glycine residue (G) at the N-terminal was reacted with the COOH-QDs. It was synthesized manually using in situ neutralization cycles for Boc-solid-phase-peptide synthesis (Boc-SPPS) following procedures described in the literature.[85] Briefly, the synthesis was carried out using 0.2 mmol of MBHA resin (4-methylbenzhydrylamine, 0.40 mmol/g), 1.0 mmol of amino acid, 1.0 mmol of HCTU (1*H*-benzotriazolium 1-[bis(dimethyl-amino)methylene]-5-chloro-hexa-fluorophosphate (1-),3-oxide in a 0.4 M solution in DMF), and 1.5 mmol of DIEA (*N*,*N*-diisopropylethylamine). Coupling times were 20 min. Following chain assembly, the peptide was cleaved from the resin with HF and 10% of anisole for 1 h at 0 °C.

Labeling of the peptide with sulfo-Cy3 dye through cysteine and maleimide reaction has been described in the Supporting Information. Here, we provide the details for conjugating 5% COOH-QDs and peptide-Cy3 using carbodiimide chemistry. Briefly, in a scintillation vial, 5% COOH-QDs (6.6 μM, 38 μL) were diluted in 10 mM PB (pH 6.5, 72 μL) and mixed with EDC (5.2 mM in 10 mM pH 6.5 PB, 40 μL). The reaction mixture was stirred for 1 h at room temperature (in the dark), followed by the addition of NHS (8.7 mM in 10 mM pH 8.7 PB, 47 μL) and a solution of Cy3-labeled peptide (529 μM, 25 μL) in DMSO. 10 mM PB (pH 8.7, 278 μL) was added to render the mixture basic. The reaction mixture was left stirring for 5 h at room temperature, and the conjugates were purified using a PD-10 desalting column. The first eluted fraction (∼400 μL, containing the conjugates) was collected and characterized using absorption and fluorescence spectroscopy. Conjugation of peptide-Cy3 to 10% COOH-QDs was carried out following the same protocol, except that the amount of coupling reagent and peptide-Cy3 was doubled to compensate for the higher number of carboxyl groups per QD and to maintain the same molar ratio between acid groups and target peptide-Cy3 as above. We also prepared control dispersions by reacting QDs photoligated with 100%-methoxy terminated ligands with Cy3-labeled peptide at similar reagent concentrations. The samples were purified using a PD-10

DOI: 10.1021/jacs.5b10359
J. Am. Chem. Soc. 2015, 137, 16084−16097

desalting column, and the first collected fraction was analyzed using absorption and fluorescence spectroscopy.

■ ASSOCIATED CONTENT

Supporting Information

The Supporting Information is available free of charge on the ACS Publications website at DOI: 10.1021/jacs.5b10359.

Additional experimental details, additional absorption and emission of QDs, synthesis of the peptide-Cy3, FRET analysis, and ^{1}H NMR spectra of the compounds (PDF)

■ AUTHOR INFORMATION

Corresponding Author

*mattoussi@chem.fsu.edu

Notes

The authors declare no competing financial interest.

■ ACKNOWLEDGMENTS

We thank FSU and the National Science Foundation for financial support (NSF-CHE nos. 1508501 and 1058957).

■ REFERENCES

(1) Chan, W. C. W.; Nie, S. M. *Science* **1998**, *281*, 2016.
(2) Bruchez, M.; Moronne, M.; Gin, P.; Weiss, S.; Alivisatos, A. P. *Science* **1998**, *281*, 2013.
(3) Alivisatos, P. *Nat. Biotechnol.* **2004**, *22*, 47.
(4) Kim, S.; Lim, Y.; Soltesz, E.; De Grand, A.; Lee, J.; Nakayama, A.; Parker, J.; Mihaljevic, T.; Laurence, R.; Dor, D.; Cohn, L.; Bawendi, M.; Frangioni, J. *Nat. Biotechnol.* **2004**, *22*, 93.
(5) Michalet, X.; Pinaud, F.; Bentolila, L.; Tsay, J.; Doose, S.; Li, J.; Sundaresan, G.; Wu, A.; Gambhir, S.; Weiss, S. *Science* **2005**, *307*, 538.
(6) El-Sayed, I. H.; Huang, X. H.; El-Sayed, M. A. *Nano Lett.* **2005**, *5*, 829.
(7) Medintz, I.; Uyeda, H.; Goldman, E.; Mattoussi, H. *Nat. Mater.* **2005**, *4*, 435.
(8) Chithrani, B. D.; Ghazani, A. A.; Chan, W. C. W. *Nano Lett.* **2006**, *6*, 662.
(9) Huang, X. H.; El-Sayed, I. H.; Qian, W.; El-Sayed, M. A. *J. Am. Chem. Soc.* **2006**, *128*, 2115.
(10) Murphy, C. J.; Gole, A. M.; Stone, J. W.; Sisco, P. N.; Alkilany, A. M.; Goldsmith, E. C.; Baxter, S. C. *Acc. Chem. Res.* **2008**, *41*, 1721.
(11) Ghosh, P.; Han, G.; De, M.; Kim, C. K.; Rotello, V. M. *Adv. Drug Delivery Rev.* **2008**, *60*, 1307.
(12) You, C. J.; Wilmes, S.; Beutel, O.; Lochte, S.; Podoplelowa, Y.; Roder, F.; Richter, C.; Seine, T.; Schaible, D.; Uze, G.; Clarke, S.; Pinaud, F.; Dahan, M.; Piehler, J. *Angew. Chem., Int. Ed.* **2010**, *49*, 4108.
(13) Pinaud, F.; Clarke, S.; Sittner, A.; Dahan, M. *Nat. Methods* **2010**, *7*, 275.
(14) Mattoussi, H.; Palui, G.; Na, H. B. *Adv. Drug Delivery Rev.* **2012**, *64*, 138.
(15) Weintraub, K. *Nature* **2013**, *495*, S14.
(16) Cai, E.; Ge, P.; Lee, S. H.; Jeyifous, O.; Wang, Y.; Liu, Y.; Wilson, K. M.; Lim, S. J.; Baird, M. A.; Stone, J. E.; Lee, K. Y.; Davidson, M. W.; Chung, H. J.; Schulten, K.; Smith, A. M.; Green, W. N.; Selvin, P. R. *Angew. Chem., Int. Ed.* **2014**, *53*, 12484.
(17) Howes, P. D.; Chandrawati, R.; Stevens, M. M. *Science* **2014**, *346*, 6205.
(18) Rana, S.; Le, N. D. B.; Mout, R.; Saha, K.; Tonga, G. Y.; Bain, R. E. S.; Miranda, O. R.; Rotello, C. M.; Rotello, V. M. *Nat. Nanotechnol.* **2014**, *10*, 65.
(19) Mie, G. *Ann. Phys.* **1908**, *25*, 377.
(20) Jana, N. R.; Gearheart, L.; Murphy, C. J. *J. Phys. Chem. B* **2001**, *105*, 4065.
(21) Kelly, K. L.; Coronado, E.; Zhao, L. L.; Schatz, G. C. *J. Phys. Chem. B* **2003**, *107*, 668.
(22) Gole, A.; Murphy, C. J. *Chem. Mater.* **2005**, *17*, 1325.
(23) Liz-Marzan, L. M. *Langmuir* **2006**, *22*, 32.
(24) Jain, P. K.; Lee, K. S.; El-Sayed, I. H.; El-Sayed, M. A. *J. Phys. Chem. B* **2006**, *110*, 7238.
(25) Jaiswal, J. K.; Mattoussi, H.; Mauro, J. M.; Simon, S. M. *Nat. Biotechnol.* **2002**, *21*, 47.
(26) Murray, C. B.; K, C. R.; Bawendi, M. G. *Annu. Rev. Mater. Sci.* **2000**, *30*, 545.
(27) Talapin, D. V.; Lee, J. S.; Kovalenko, M. V.; Shevchenko, E. V. *Chem. Rev.* **2010**, *110*, 389.
(28) Resch-Genger, U.; Grabolle, M.; Cavaliere-Jaricot, S.; Nitschke, R.; Nann, T. *Nat. Methods* **2008**, *5*, 763.
(29) Larson, D. R.; Zipfel, W. R.; Williams, R. M.; Clark, S. W.; Bruchez, M. P.; Wise, F. W.; Webb, W. W. *Science* **2003**, *300*, 1434.
(30) Talapin, D. V.; Rogach, A. L.; Kornowski, A.; Haase, M.; Weller, H. *Nano Lett.* **2001**, *1*, 207.
(31) Reiss, P.; Bleuse, J.; Pron, A. *Nano Lett.* **2002**, *2*, 781.
(32) Peng, Z. A.; Peng, X. G. *J. Am. Chem. Soc.* **2001**, *123*, 183.
(33) Murray, C. B.; Norris, D. J.; Bawendi, M. G. *J. Am. Chem. Soc.* **1993**, *115*, 8706.
(34) Hines, M. A.; Guyot-Sionnest, P. *J. Phys. Chem.* **1996**, *100*, 468.
(35) Dabbousi, B. O.; RodriguezViejo, J.; Mikulec, F. V.; Heine, J. R.; Mattoussi, H.; Ober, R.; Jensen, K. F.; Bawendi, M. G. *J. Phys. Chem. B* **1997**, *101*, 9463.
(36) Reiss, P.; Protiere, M.; Li, L. *Small* **2009**, *5*, 154.
(37) Sapsford, K. E.; Algar, W. R.; Berti, L.; Gemmill, K. B.; Casey, B. J.; Oh, E.; Stewart, M. H.; Medintz, I. L. *Chem. Rev.* **2013**, *113*, 1904.
(38) Nam, J.; Won, N.; Bang, J.; Jin, H.; Park, J.; Jung, S.; Jung, S.; Park, Y.; Kim, S. *Adv. Drug Delivery Rev.* **2013**, *65*, 622.
(39) Tyrakowski, C. M.; Snee, P. T. *Phys. Chem. Chem. Phys.* **2014**, *16*, 837.
(40) Liu, D.; Snee, P. T. *ACS Nano* **2011**, *5*, 546.
(41) Giovanelli, E.; Muro, E.; Sitbon, G.; Hanafi, M.; Pons, T.; Dubertret, B.; Lequeux, N. *Langmuir* **2012**, *28*, 15177.
(42) Yi, D. K.; Selvan, S. T.; Lee, S. S.; Papaefthymiou, G. C.; Kundaliya, D.; Ying, J. Y. *J. Am. Chem. Soc.* **2005**, *127*, 4990.
(43) Gerion, D.; Pinaud, F.; Williams, S. C.; Parak, W. J.; Zanchet, D.; Weiss, S.; Alivisatos, A. P. *J. Phys. Chem. B* **2001**, *105*, 8861.
(44) Dubertret, B.; Skourides, P.; Norris, D. J.; Noireaux, V.; Brivanlou, A. H.; Libchaber, A. *Science* **2002**, *298*, 1759.
(45) Susumu, K.; Uyeda, H. T.; Medintz, I. L.; Pons, T.; Delehanty, J. B.; Mattoussi, H. *J. Am. Chem. Soc.* **2007**, *129*, 13987.
(46) Liu, W. H.; Greytak, A. B.; Lee, J.; Wong, C. R.; Park, J.; Marshall, L. F.; Jiang, W.; Curtin, P. N.; Ting, A. Y.; Nocera, D. G.; Fukumura, D.; Jain, R. K.; Bawendi, M. G. *J. Am. Chem. Soc.* **2010**, *132*, 472.
(47) Snee, P. T.; Somers, R. C.; Nair, G.; Zimmer, J. P.; Bawendi, M. G.; Nocera, D. G. *J. Am. Chem. Soc.* **2006**, *128*, 13320.
(48) Yildiz, I.; McCaughan, B.; Cruickshank, S. F.; Callan, J. F.; Raymo, F. M. *Langmuir* **2009**, *25*, 7090.
(49) Mei, B. C.; Susumu, K.; Medintz, I. L.; Delehanty, J. B.; Mountziaris, T. J.; Mattoussi, H. *J. Mater. Chem.* **2008**, *18*, 4949.
(50) Uyeda, H. T.; Medintz, I. L.; Jaiswal, J. K.; Simon, S. M.; Mattoussi, H. *J. Am. Chem. Soc.* **2005**, *127*, 3870.
(51) Muro, E.; Fragola, A.; Pons, T.; Lequeux, N.; Ioannou, A.; Skourides, P.; Dubertret, B. *Small* **2012**, *8*, 1029.
(52) Palui, G.; Aldeek, F.; Wang, W. T.; Mattoussi, H. *Chem. Soc. Rev.* **2015**, *44*, 193.
(53) Pellegrino, T.; Manna, L.; Kudera, S.; Liedl, T.; Koktysh, D.; Rogach, A. L.; Keller, S.; Radler, J.; Natile, G.; Parak, W. J. *Nano Lett.* **2004**, *4*, 703.
(54) Susumu, K.; Mei, B. C.; Mattoussi, H. *Nat. Protoc.* **2009**, *4*, 424.
(55) Yildiz, I.; Deniz, E.; McCaughan, B.; Cruickshank, S. F.; Callan, J. F.; Raymo, F. M. *Langmuir* **2010**, *26*, 11503.
(56) Muro, E.; Pons, T.; Lequeux, N.; Fragola, A.; Sanson, N.; Lenkei, Z.; Dubertret, B. *J. Am. Chem. Soc.* **2010**, *132*, 4556.

DOI: 10.1021/jacs.5b10359
J. Am. Chem. Soc. 2015, 137, 16084−16097

(57) Zhang, P.; Liu, S.; Gao, D.; Hu, D.; Gong, P.; Sheng, Z.; Deng, J.; Ma, Y.; Cai, L. *J. Am. Chem. Soc.* **2012**, *134*, 8388.
(58) Susumu, K.; Oh, E.; Delehanty, J. B.; Pinaud, F.; Gemmill, K. B.; Walper, S.; Breger, J.; Schroeder, M. J.; Stewart, M. H.; Jain, V.; Whitaker, C. M.; Huston, A. L.; Medintz, I. L. *Chem. Mater.* **2014**, *26*, 5327.
(59) Wang, W.; Kapur, A.; Ji, X.; Safi, M.; Palui, G.; Palomo, V.; Dawson, P. E.; Mattoussi, H. *J. Am. Chem. Soc.* **2015**, *137*, 5438.
(60) Liu, W.; Howarth, M.; Greytak, A. B.; Zheng, Y.; Nocera, D. G.; Ting, A. Y.; Bawendi, M. G. *J. Am. Chem. Soc.* **2008**, *130*, 1274.
(61) Viswanath, A.; Shen, Y.; Green, A. N.; Tan, R.; Greytak, A. B.; Benicewicz, B. C. *Macromolecules* **2014**, *47*, 8137.
(62) Mattoussi, H.; Mauro, J. M.; Goldman, E. R.; Anderson, G. P.; Sundar, V. C.; Mikulec, F. V.; Bawendi, M. G. *J. Am. Chem. Soc.* **2000**, *122*, 12142.
(63) Gravel, E.; Tanguy, C.; Cassette, E.; Pons, T.; Knittel, F.; Bernards, N.; Garofalakis, A.; Duconge, F.; Dubertret, B.; Doris, E. *Chem. Sci.* **2013**, *4*, 411.
(64) Stewart, M. H.; Susumu, K.; Mei, B. C.; Medintz, I. L.; Delehanty, J. B.; Blanco-Canosa, J. B.; Dawson, P. E.; Mattoussi, H. *J. Am. Chem. Soc.* **2010**, *132*, 9804.
(65) Zhan, N.; Palui, G.; Grise, H.; Tang, H.; Alabugin, I.; Mattoussi, H. *ACS Appl. Mater. Interfaces* **2013**, *5*, 2861.
(66) Oh, E.; Susumu, K.; Goswami, R.; Mattoussi, H. *Langmuir* **2010**, *26*, 7604.
(67) Chen, X. J.; Lawrence, J.; Parelkar, S.; Emrick, T. *Macromolecules* **2013**, *46*, 119.
(68) Mei, B. C.; Oh, E.; Susumu, K.; Farrell, D.; Mountziaris, T. J.; Mattoussi, H. *Langmuir* **2009**, *25*, 10604.
(69) Palui, G.; Avellini, T.; Zhan, N.; Pan, F.; Gray, D.; Alabugin, I.; Mattoussi, H. *J. Am. Chem. Soc.* **2012**, *134*, 16370.
(70) Zhan, N. Q.; Palui, G.; Safi, M.; Ji, X.; Mattoussi, H. *J. Am. Chem. Soc.* **2013**, *135*, 13786.
(71) Mei, B. C.; Susumu, K.; Medintz, I. L.; Mattoussi, H. *Nat. Protoc.* **2009**, *4*, 412.
(72) Isaacs, S. R.; Cutler, E. C.; Park, J. S.; Lee, T. R.; Shon, Y. S. *Langmuir* **2005**, *21*, 5689.
(73) Daniels, T. R.; Delgado, T.; Rodriguez, J. A.; Helguera, G.; Penichet, M. L. *Clin. Immunol.* **2006**, *121*, 144.
(74) Lowe, S. B.; Dick, J. A. G.; Cohen, B. E.; Stevens, M. M. *ACS Nano* **2012**, *6*, 851.
(75) Silvi, S.; Credi, A. *Chem. Soc. Rev.* **2015**, *44*, 4275.
(76) Medintz, I. L.; Stewart, M. H.; Trammell, S. A.; Susumu, K.; Delehanty, J. B.; Mei, B. C.; Melinger, J. S.; Blanco-Canosa, J. B.; Dawson, P. E.; Mattoussi, H. *Nat. Mater.* **2010**, *9*, 676.
(77) Chung, E. Y.; Ochs, C. J.; Wang, Y.; Lei, L.; Qin, Q.; Smith, A. M.; Strongin, A. Y.; Kamm, R.; Qi, Y.-X.; Lu, S.; Wang, Y. *Nano Lett.* **2015**, *15*, 5025.
(78) Mattoussi, H.; Cumming, A. W.; Murray, C. B.; Bawendi, M. G.; Ober, R. *Phys. Rev. B: Condens. Matter Mater. Phys.* **1998**, *58*, 7850.
(79) Leatherdale, C. A.; Woo, W. K.; Mikulec, F. V.; Bawendi, M. G. *J. Phys. Chem. B* **2002**, *106*, 7619.
(80) Clapp, A. R.; Medintz, I. L.; Mauro, J. M.; Fisher, B. R.; Bawendi, M. G.; Mattoussi, H. *J. Am. Chem. Soc.* **2004**, *126*, 301.
(81) Palui, G.; Na, H. B.; Mattoussi, H. *Langmuir* **2012**, *28*, 2761.
(82) Susumu, K.; Oh, E.; Delehanty, J. B.; Blanco-Canosa, J. B.; Johnson, B. J.; Jain, V.; Hervey, W. J.; Algar, W. R.; Boeneman, K.; Dawson, P. E.; Medintz, I. L. *J. Am. Chem. Soc.* **2011**, *133*, 9480.
(83) Yu, W. W.; Peng, X. G. *Angew. Chem., Int. Ed.* **2002**, *41*, 2368.
(84) Ojea-Jiménez, I.; García-Fernández, L.; Lorenzo, J.; Puntes, V. F. *ACS Nano* **2012**, *6*, 7692.
(85) Schnolzer, M.; Alewood, P.; Jones, A.; Alewood, D.; Kent, S. B. H. *Int. J. Pept. Protein Res.* **1992**, *40*, 180.

DOI: 10.1021/jacs.5b10359
J. Am. Chem. Soc. 2015, 137, 16084−16097